

Stochastic Discontinuous Galerkin Methods for Robust Deterministic Control of Convection Diffusion Equations with Uncertain Coefficients

Pelin Çiloğlu¹ and Hamdullah Yücel^{1*}

¹Institute of Applied Mathematics, Middle East Technical
University, Ankara, 06800, Turkey.

*Corresponding author(s). E-mail(s): yucelh@metu.edu.tr;
Contributing authors: pciloglu@metu.edu.tr;

Abstract

We investigate a numerical behaviour of robust deterministic optimal control problem subject to a convection diffusion equation containing uncertain inputs. Stochastic Galerkin approach, turning the original optimization problem containing uncertainties into a large system of deterministic problems, is applied to discretize the stochastic domain, while a discontinuous Galerkin method is preferred for the spatial discretization due to its better convergence behaviour for optimization problems governed by convection dominated PDEs. Error analysis is done for the state and adjoint variables in the energy norm, while the estimates of deterministic control is obtained in the \mathbf{L}^2 -norm. Large matrix system emerging from the stochastic Galerkin method is addressed by the low-rank version of GMRES method, which reduces both the computational complexity and the memory requirements by employing Kronecker-product structure of the obtained linear system. Benchmark examples with and without control constraints are presented to illustrate the efficiency of the proposed methodology.

Keywords: PDE-constrained optimization, uncertainty quantification, stochastic discontinuous Galerkin, error estimates, low-rank approximation

MSC Classification: 35R60 , 49J20 , 60H15 , 60H35

1 Introduction

In many phenomena in physics or engineering applications, certain parameters of a model are optimized in order to reach the desired target, for instance, the location where the oil is inserted into the medium, the temperature of a melting/heating process, or the shape of the aircraft wings. Such real-world phenomena can be modelled as optimal control problems or optimization problems with PDE constraints. However, in reality, the input parameters of these simulations, such as the wind speed or material properties, are not often known due to the missing information or inherent variability in the problem; see, e.g., [1]. Therefore, in the last decade, the idea of uncertainty quantification, i.e., quantifying the effects of uncertainty on the result of a computation, has become a powerful tool for modeling physical phenomena in the scientific community.

PDE-constraint optimization problems with uncertainty have been studied in various formulations in the literature, such as mean-based control [2, 3], pathwise control [4, 5], average control [6, 7], robust deterministic control [8–13], and robust stochastic control [14–17]. Robust deterministic control is more practical and realistic since randomness cannot be observed during the design of the control. Therefore, we are here interested with the following robust deterministic control problem

$$\min_{u \in \mathcal{U}^{ad}} \mathcal{J}(y, u) := \frac{1}{2} \|y - y^d\|_{\mathcal{X}}^2 + \frac{\gamma}{2} \|\text{std}(y)\|_{\mathcal{W}}^2 + \frac{\mu}{2} \|u\|_{\mathcal{U}}^2 \quad (1.1)$$

governed by

$$\mathcal{S}(y(\mathbf{x}, \omega)) = f(\mathbf{x}) + u(\mathbf{x}) \quad \text{in } \mathcal{D} \times \Omega, \quad (1.2a)$$

$$y(\mathbf{x}, \omega) = y_{DB}(\mathbf{x}) \quad \text{on } \partial\mathcal{D} \times \Omega, \quad (1.2b)$$

where $\mathcal{S} : \mathcal{Y} \rightarrow \mathcal{Y}'$ is a linear operator that contains uncertain parameters, $\mathcal{D} \subset \mathbb{R}^2$ is a convex bounded polygonal set with a Lipschitz boundary $\partial\mathcal{D}$, and Ω is a sample space of events. The cost functional including a risk penalization via the standard deviation $\text{std}(y)$ is denoted by $\mathcal{J}(y, u)$. The first term in (1.1) is a measure of the distance between the state variable y and the desired state y^d in terms of expectation of $y - y^d$. Without loss of generality, we assume that the state $y \in \mathcal{Y}$ is a random field, whereas the desired state $y^d \in \mathcal{Y}$ is modelled deterministically. The second term measures the standard deviation of y , which is added since it is desirable to have a control for which the state is more accurately known, leading to a risk averse optimum. The last term corresponds to distributive deterministic control. The constant $\mu > 0$ is a positive regularization parameter of the control u , whereas $\gamma \geq 0$ is a risk-aversion parameter. Deterministic source function and Dirichlet boundary conditions are denoted by f and y_{DB} , respectively. We note that the cost functional \mathcal{J} is a deterministic quantity although it contains uncertain inputs.

Further, the closed convex admissible set in the control space \mathcal{U} is defined by

$$\mathcal{U}^{ad} := \{u \in \mathcal{U} : u_a \leq u(\mathbf{x}) \leq u_b, \quad \forall \mathbf{x} \in \mathcal{D}\}, \quad (1.3)$$

where constants $u_a, u_b \in \mathbb{R}$ with $u_a \leq u_b$.

Finding an approximate solution for the optimization problems containing uncertainty (1.1)–(1.2) is extremely challenging and requires much more computational resources than the ones in the deterministic setting. In the literature, there exist various competing methods to solve such kinds of problem, for instance, Monte Carlo (MC) [5, 18, 19], stochastic collocation method (SCM) [13, 17, 20, 21], and stochastic Galerkin method (SGM) [9, 12, 13, 22, 23]. Although the MC method is popular for its simplicity, natural parallelization, and broad applications, it features slow convergence, which does not depend on the number of uncertain parameters [24, 25]. For the SCMs, the crucial issue is how to construct the set of collocation points appropriately because the choice of the collocation points determines the efficiency of the method. In contrast to the MC approach and the SCM, the SGM is a nonsampling technique, which transforms the problem into a large system of deterministic problems. As in the classic (deterministic) Galerkin method, the idea behind the SGM is to seek a solution for the model equation such that the residue is orthogonal to the space of polynomials. Since the random process is expressed as an expansion with the help of orthogonal polynomials, the SGM is considered as a variant of the generalized polynomial chaos approximation [26–28] as the stochastic collocation method. An important feature of the SGM is the separation of the spatial and stochastic variables, which allows a reuse of established numerical techniques. The results obtained in [13] also show that the SGM generally displays superior performance compared to the SCM for the robust deterministic control problems. Within the framework of the aforementioned features, the stochastic Galerkin method is preferred as a stochastic method in this study. On the other hand, for the discretization of the spatial domain, we use a discontinuous Galerkin method due to its better convergence behaviour for the optimization problems governed by convection dominated PDEs; see, e.g., [29–31]. We also refer to [32, 33] and references therein for more details on the discontinuous Galerkin methods.

In spite of these nice properties exhibited by the stochastic discontinuous Galerkin method, the dimension of the resulting linear system increases rapidly, called as the curse of dimensionality. As a remedy, we apply a low-rank variant of generalized minimal residual (GMRES) method [34] with a suitable preconditioner. With the help of a Kronecker-product structure of the obtained large matrices, we reduce both the computational complexity and memory requirements; see, e.g., [35–37]. Low-rank approximation of the optimal control problems with uncertain terms have been also studied in [14, 38, 39] for unconstrained control problems and in [40] for control constraint problems. In the aforementioned studies, randomness is generally defined on the diffusion parameter; however, we here consider the randomness on diffusion or convection parameters by applying the discontinuous Galerkin method in the

spatial domain. In addition, according to the best of our knowledge, a low-rank approximation of the optimal control problems governed by convection dominated equations containing randomness has not been discussed before in the setting of discontinuous Galerkin discretization in the spatial domain.

We organize our paper by first discussing the existence of the solution in the next section. In Section 3, we reduce the problem into finite dimensional setting via Karhunen–Loève (KL) expansion, stochastic Galerkin method, and symmetric interior penalty Galerkin method. Error analyses are done in Section 4. In Section 5, we construct the matrix formulation of the underlying optimization problem by proceeding the optimize-then-discretize approach, and then discuss implementation of the low-rank GMRES solver. Results of the numerical experiments are provided in Section 6 to illustrate the efficiency of the proposed methodology. Finally, we end the paper with some conclusions and discussions in Section 7.

2 Existence and uniqueness of the solution

Let Ω be a sample space of events, $\mathcal{F} \subset 2^\Omega$ denotes a σ -algebra, and \mathbb{P} is the associated probability measure that maps the events in \mathcal{F} to probabilities in $[0, 1]$. A generic random field η on the probability space $(\Omega, \mathcal{F}, \mathbb{P})$ is denoted by $\eta(\mathbf{x}, \omega) : \mathcal{D} \times \Omega \rightarrow \mathbb{R}$. For a fixed $\mathbf{x} \in \mathcal{D}$, $\eta(\mathbf{x}, \cdot)$ is a real-valued square integrable random variable $\eta(\mathbf{x}, \cdot) \in L^2(\Omega, \mathcal{F}, \mathbb{P})$, i.e.,

$$L^2(\Omega) := L^2(\Omega, \mathcal{F}, \mathbb{P}) := \{X : \Omega \rightarrow \mathbb{R} : \int_{\Omega} |X(\omega)|^2 d\mathbb{P}(\omega) < \infty\}.$$

Then, the mean $\mathbb{E}[\eta]$, the standard deviation $\text{std}(\eta)$, and the corresponding variance $\mathbb{V}(\eta)$ for any random field η , are given, respectively, by

$$\begin{aligned} \mathbb{E}[\eta] &= \int_{\Omega} \eta d\mathbb{P}(\omega), & \text{std}(\eta) &= \left[\int_{\Omega} (\eta - \mathbb{E}[\eta])^2 d\mathbb{P}(\omega) \right]^{1/2}, \\ \mathbb{V}(\eta) &= [\text{std}(\eta)]^2 = \mathbb{E}[\eta^2] - (\mathbb{E}[\eta])^2. \end{aligned}$$

Recalling the tensor-product space $H^k(\mathcal{D}) \otimes L^2(\Omega)$ equipped with the norm

$$\|\eta\|_{H^k(\mathcal{D}) \otimes L^2(\Omega)} := \left(\int_{\Omega} \|\eta(\cdot, \omega)\|_{H^k(\mathcal{D})}^2 d\mathbb{P}(\omega) \right)^{1/2} < \infty, \quad (2.1)$$

the state and control spaces are defined as follow, respectively,

$$\mathcal{Y} := H_0^1(\mathcal{D}) \otimes L^2(\Omega) \quad \text{and} \quad \mathcal{U} := L^2(\mathcal{D}).$$

We also set $\mathcal{X} := L^2(\mathcal{D}) \otimes L^2(\Omega)$ and $\mathcal{W} = L^2(\mathcal{D})$.

In order to show existence of the solution, it is assumed that the operator \mathcal{S} satisfies the following conditions:

- a) \mathcal{S} is coercive such that \mathbb{P} -a.s., $(\mathcal{S}v, v) \geq c\|v\|_{\mathcal{X}}, \forall v \in \mathcal{X}$, where c is a positive constant.
- b) $(\mathcal{S}u, v) = (u, \mathcal{S}^*v) \forall u, v \in \mathcal{X}$, where \mathcal{S}^* is the adjoint of \mathcal{S} .

By following the standard arguments in the theory of optimal control, see, e.g., [41, Theorem 1.3] and [42, Theorem 2.14], the existence and uniqueness of an optimal solution for the optimization problem (1.1)–(1.2) can be proved. With the definitions above, \mathcal{Y} and \mathcal{U} are Hilbert spaces, the functional \mathcal{J} is strictly convex, and the admissible set \mathcal{U}^{ad} is a closed and convex set. Then, according to Lion's Lemma [41, Theorem 1.3], a unique optimal control $\bar{u} \in \mathcal{U}$ exists and the variational inequality holds

$$\mathcal{J}'(\bar{u}) \cdot (v - \bar{u}) \geq 0, \quad \forall v \in \mathcal{U}^{ad}. \quad (2.2)$$

Now, we can state the first order optimality system of the optimization problem containing uncertain coefficients (1.1)–(1.2).

Theorem 2.1. *A pair (y, u) is a unique solution of the optimization problem (1.1)–(1.2) if and only if there exists an adjoint $p \in \mathcal{Y}$ such that the optimality system holds, \mathbb{P} -a.s., for the triplet $(y(u), u, p(u)) \in \mathcal{Y} \times \mathcal{U}^{ad} \times \mathcal{Y}$*

$$\mathcal{S}(y(u)) = f(\mathbf{x}) + u(\mathbf{x}), \quad (2.3a)$$

$$\mathcal{S}^*(p(u)) = y(u) - y^d + \gamma(y(u) - \mathbb{E}[y(u)]), \quad (2.3b)$$

$$(\mathbb{E}[p(u)] + \mu u, v - u) \geq 0, \quad v \in \mathcal{U}^{ad}. \quad (2.3c)$$

Proof Rewrite the objective functional \mathcal{J} as

$$\begin{aligned} \mathcal{J}(u) = & \underbrace{\frac{1}{2}\mathbb{E}\left[\int_{\mathcal{D}} \left(y(u) - y^d\right)^2 d\mathbf{x}\right]}_{\mathcal{J}_1(u)} + \underbrace{\frac{\gamma}{2}\mathbb{E}\left[\int_{\mathcal{D}} y(u)^2 d\mathbf{x}\right]}_{\mathcal{J}_2(u)} \\ & - \underbrace{\frac{\gamma}{2}\int_{\mathcal{D}} (\mathbb{E}[y(u)])^2 d\mathbf{x}}_{\mathcal{J}_3(u)} + \underbrace{\frac{\mu}{2}\int_{\mathcal{D}} u^2 d\mathbf{x}}_{\mathcal{J}_4(u)}. \end{aligned}$$

By the definition of directional derivative, we obtain that

$$\begin{aligned} \mathcal{J}'(u) \cdot (v - u) &= \mathbb{E}\left[\int_{\mathcal{D}} (y(u) - y^d)y'(u) \cdot (v - u) d\mathbf{x}\right] + \gamma\mathbb{E}\left[\int_{\mathcal{D}} y(u)y'(u) \cdot (v - u) d\mathbf{x}\right] \\ &\quad - \gamma\int_{\mathcal{D}} \mathbb{E}[y(u)]y'(u) \cdot (v - u) d\mathbf{x} + \mu\int_{\mathcal{D}} u \cdot (v - u) d\mathbf{x}. \end{aligned} \quad (2.4)$$

By well-posedness of the state equation (1.2) followed from the Lax–Milgram lemma, one can easily show that the operator \mathcal{S} is invertible so that, by taking directional derivative, one gets

$$y'(u) \cdot (v - u) = \mathcal{S}^{-1}(v - u) = y(v) - y(u).$$

Thus, (2.4) gives us

$$\mathcal{J}'(u) \cdot (v - u) = \Psi(\gamma) + \mu \int_{\mathcal{D}} u \cdot (v - u) \, d\mathbf{x}, \quad (2.5)$$

where

$$\begin{aligned} \Psi(\gamma) = & (1 + \gamma) \mathbb{E} \left[\int_{\mathcal{D}} y(u) \cdot (y(v) - y(u)) \, d\mathbf{x} \right] - \gamma \int_{\mathcal{D}} \mathbb{E}[y(u)] \cdot (y(v) - y(u)) \, d\mathbf{x} \\ & - \mathbb{E} \left[\int_{\mathcal{D}} y^d \cdot (y(v) - y(u)) \, d\mathbf{x} \right]. \end{aligned}$$

To guarantee the existence and uniqueness of the solution from Lion's Lemma [41, Theorem 1.3], we need the following requirement

$$\mathcal{J}'(u) \cdot (v - u) \geq 0. \quad (2.6)$$

Next, we introduce the adjoint state $p(u) \in \mathcal{Y}$ by

$$\mathcal{S}^*(p(u)) = y(u) - y^d + \gamma(y(u) - \mathbb{E}[y(u)]). \quad (2.7)$$

Multiplying both sides of (2.7) by $(y(v) - y(u))$, integrating over \mathcal{D} , and taking the expectation of the resulting system, we obtain

$$\begin{aligned} \mathbb{E} \left[\int_{\mathcal{D}} \mathcal{S}^*(p(u)) \cdot (y(v) - y(u)) \, d\mathbf{x} \right] &= \mathbb{E} \left[\int_{\mathcal{D}} p(u) \cdot (\mathcal{S}(y(v)) - \mathcal{S}(y(u))) \, d\mathbf{x} \right] \\ &= \mathbb{E} \left[\int_{\mathcal{D}} p(u) \cdot (v - u) \, d\mathbf{x} \right] \\ &= \Psi(\gamma). \end{aligned} \quad (2.8)$$

Inserting (2.8) into (2.5) and combining with (2.6) give us

$$\mathcal{J}'(u) \cdot (v - u) = (\mathbb{E}[p(u)] + \mu u, v - u) \geq 0, \quad (2.9)$$

which is the desired result. \square

In this study, we consider \mathcal{S} as the convection–diffusion operator

$$\mathcal{S} := -\nabla \cdot (a(\mathbf{x}, \omega) \nabla) + \mathbf{b}(\mathbf{x}, \omega) \cdot \nabla, \quad (2.10)$$

which turns the state equation (1.2) into

$$-\nabla \cdot (a(\mathbf{x}, \omega) \nabla y) + \mathbf{b}(\mathbf{x}, \omega) \cdot \nabla y = f + u \quad \text{in } \mathcal{D} \times \Omega, \quad (2.11a)$$

$$y = y_{DB} \quad \text{on } \partial\mathcal{D} \times \Omega, \quad (2.11b)$$

where $a : (\mathcal{D} \times \Omega) \rightarrow \mathbb{R}$ and $\mathbf{b} : (\mathcal{D} \times \Omega) \rightarrow \mathbb{R}^2$ are random diffusivity and velocity coefficients, respectively, which is assumed to have continuous and bounded covariance functions. In addition, we make the following assumptions on the uncertain coefficients:

- i) $\exists a_{min}, a_{max}$ such that for almost every $(\mathbf{x}, \omega) \in \mathcal{D} \times \Omega$, $0 < a_{min} \leq a(\mathbf{x}, \omega) \leq a_{max} < \infty$. In addition, $a(\mathbf{x}, \omega)$ has a uniformly bounded and continuous first derivatives.
- ii) The velocity coefficient \mathbf{b} satisfies $\mathbf{b}(\cdot, \omega) \in (L^\infty(\overline{\mathcal{D}}))^2$ for a.e. $\omega \in \Omega$ and $\nabla \cdot \mathbf{b}(\mathbf{x}, \omega) = 0$.

Then, the well-posedness of the state equation (2.11) can be shown by following the classical Lax–Milgram lemma; see, e.g., [43, 44].

Now, we give the corresponding weak formulation of the optimization problem containing uncertainty (1.1)–(1.2) as follows

$$\begin{aligned} \min_{u \in \mathcal{U}^{ad}} \mathcal{J}(u) &= \frac{1}{2} \mathbb{E} \left[\int_{\mathcal{D}} (y(u) - y^d)^2 d\mathbf{x} \right] + \frac{\gamma}{2} \mathbb{E} \left[\int_{\mathcal{D}} (y(u) - \mathbb{E}[y(u)])^2 d\mathbf{x} \right] \\ &\quad + \frac{\mu}{2} \int_{\mathcal{D}} u^2 d\mathbf{x} \end{aligned} \quad (2.12)$$

governed by

$$a[y, v] + b[u, v] = [f, v], \quad v \in \mathcal{Y}, \quad (2.13)$$

where

$$\begin{aligned} a[y, v] &= \mathbb{E} \left[\int_{\mathcal{D}} (a(\mathbf{x}, \omega) \nabla y \cdot \nabla v + \mathbf{b}(\mathbf{x}, \omega) \cdot \nabla y v) d\mathbf{x} \right], \quad \forall y, v \in \mathcal{Y}, \\ b[u, v] &= -\mathbb{E} \left[\int_{\mathcal{D}} uv d\mathbf{x} \right] \quad \text{and} \quad [f, v] = \mathbb{E} \left[\int_{\mathcal{D}} f v d\mathbf{x} \right], \quad \forall u \in \mathcal{U}, v \in \mathcal{Y}. \end{aligned}$$

Moreover, the optimality system in (2.3) can be stated in the weak formulation as follows:

$$a[y, v] + b[u, v] = [f, v], \quad v \in \mathcal{Y}, \quad (2.15a)$$

$$a[q, p] = [y - y^d, q] + \gamma[y - \mathbb{E}[y], q], \quad q \in \mathcal{Y}, \quad (2.15b)$$

$$(\mathbb{E}[p] + \mu u, w - u) \geq 0, \quad w \in \mathcal{U}^{ad}, \quad (2.15c)$$

where the adjoint $p \in \mathcal{Y}$ solves the following convection diffusion equation containing uncertain inputs

$$-\nabla \cdot (a(\mathbf{x}, \omega) \nabla p) - \mathbf{b}(\mathbf{x}, \omega) \cdot \nabla p = (y - y^d) + \gamma(y - \mathbb{E}[y]) \text{ in } \mathcal{D} \times \Omega, \quad (2.16a)$$

$$p = 0 \quad \text{on } \partial\mathcal{D} \times \Omega. \quad (2.16b)$$

In the following, we introduce the techniques, that is, Karhunen–Lòève (KL) expansion, stochastic Galerkin, and discontinuous Galerkin method, to recast the infinite-dimensional model problem (2.12)–(2.13) into the finite dimensional.

3 Finite dimensional representation

3.1 Finite representation of stochastic fields

To solve (2.12)–(2.13) numerically, it is needed to reduce the stochastic process into finite mutually uncorrelated random variables. Therefore, the coefficients $a(\mathbf{x}, \omega)$ and $\mathbf{b}(\mathbf{x}, \omega)$ are approximated by finite uncorrelated components $\{\xi_i(\omega)\}_{i=1}^{N \in \mathbb{N}}$, called as finite dimensional noise [43, 45]. Introducing the probability density functions of $\{\xi_i(\omega)\}_{i=1}^{N \in \mathbb{N}}$ denoted by $\rho_i : \Gamma_i \rightarrow [0, 1]$ with a bounded interval $\Gamma_i = \xi_i(\Omega) \in \mathbb{R}$, the probability space $(\Omega, \mathcal{F}, \mathbb{P})$ is replaced by $(\Gamma, \mathcal{B}(\Gamma), \rho(\xi)d\xi)$, where Γ represents the support of such probability density, $\mathcal{B}(\Gamma)$ is a Borel σ -algebra, and $\rho(\xi)d\xi$ corresponds to the distribution measure of ξ . Moreover, $\rho(\xi)$ denotes the joint probability density function. Hence, we can state the tensor-product space $H^k(\mathcal{D}) \otimes L^2(\Gamma)$ endowed with the following norm

$$\|\eta\|_{H^k(\mathcal{D}) \otimes L^2(\Gamma)} := \left(\int_{\Gamma} \|\eta(\cdot, \xi)\|_{H^k(\mathcal{D})}^2 \rho(\xi) d\xi \right)^{1/2} < \infty. \quad (3.1)$$

Following the well-known KL expansion [46, 47], a random field η having a continuous covariance function as follows

$$\mathbb{C}_{\eta}(\mathbf{x}, \mathbf{y}) := \int_{\Omega} (\eta(\mathbf{x}, \cdot) - \bar{\eta}(\mathbf{x}))(\eta(\mathbf{y}, \cdot) - \bar{\eta}(\mathbf{y})) d\mathbb{P}(\omega) \quad (3.2)$$

admits a proper orthogonal decomposition

$$\eta(\mathbf{x}, \omega) = \bar{\eta}(\mathbf{x}) + \kappa \sum_{k=1}^{\infty} \sqrt{\lambda_k} \phi_k(\mathbf{x}) \xi_k(\omega), \quad (3.3)$$

where $\bar{\eta}(\mathbf{x})$ and κ are mean and standard deviation of η , respectively, and $\xi := \{\xi_1, \xi_2, \dots\}$ are uncorrelated random variables. The pair $\{\lambda_k, \phi_k\}$ is a set of the eigenvalues and eigenfunctions of the corresponding covariance operator \mathcal{C}_{η} . Then, we approximate $\eta(\mathbf{x}, \omega)$ by truncating its KL expansion of the form

$$\eta(\mathbf{x}, \omega) \approx \eta_N(\mathbf{x}, \omega) := \bar{\eta}(\mathbf{x}) + \kappa \sum_{k=1}^N \sqrt{\lambda_k} \phi_k(\mathbf{x}) \xi_k(\omega). \quad (3.4)$$

The truncated KL expansion (3.4) is a finite representation of the random field $\eta(\mathbf{x}, \omega)$ in the sense that the mean-square error of approximation is minimized; see, e.g., [48]. To guarantee the positivity of the truncated KL expansion (3.4) for the diffusivity coefficient $a(\mathbf{x}, \omega)$, it is also assumed that the mean of random coefficient exhibits a stronger dominance; see, e.g., [49].

By the assumption on the finite dimensional and Doob–Dynkin lemma [50], the solution of (2.11) can be expressed in the finite dimensional stochastic space, that means, $y(\mathbf{x}, \xi(\omega)) \in \mathcal{Y}_{\rho} = L^2(H_0^1(\mathcal{D}); \Gamma)$ with $\xi =$

$(\xi_1(\omega), \dots, \xi_N(\omega))$. Then, setting $\tilde{\mathbb{E}}[y] = \int_{\Gamma} y \rho(\xi) d\xi$, the optimization problem (2.12)-(2.13) becomes

$$\begin{aligned} \min_{u \in \mathcal{U}^{ad}} \mathcal{J}(u) &= \frac{1}{2} \tilde{\mathbb{E}} \left[\int_{\mathcal{D}} (y(u) - y^d)^2 d\mathbf{x} \right] + \frac{\gamma}{2} \tilde{\mathbb{E}} \left[\int_{\mathcal{D}} (y(u) - \tilde{\mathbb{E}}[y(u)])^2 d\mathbf{x} \right] \\ &\quad + \frac{\mu}{2} \int_{\mathcal{D}} u^2 d\mathbf{x} \end{aligned} \quad (3.5)$$

subject to

$$a[y, v]_{\rho} + b[u, v]_{\rho} = [f, v]_{\rho}, \quad \forall v \in \mathcal{Y}_{\rho}, \quad (3.6)$$

where

$$a[y, v]_{\rho} = \int_{\Gamma} \int_{\mathcal{D}} (a(\mathbf{x}, \xi) \nabla y \cdot \nabla v + \mathbf{b}(\mathbf{x}, \xi) \cdot \nabla y v) d\mathbf{x} \rho(\xi) d\xi, \quad \forall y, v \in \mathcal{Y}_{\rho}, \quad (3.7a)$$

$$b[u, v]_{\rho} = - \int_{\Gamma} \int_{\mathcal{D}} uv d\mathbf{x} \rho(\xi) d\xi, \quad \forall u \in \mathcal{U}, v \in \mathcal{Y}_{\rho}, \quad (3.7b)$$

$$[f, v]_{\rho} = \int_{\Gamma} \int_{\mathcal{D}} fv d\mathbf{x} \rho(\xi) d\xi, \quad \forall v \in \mathcal{Y}_{\rho}. \quad (3.7c)$$

Then, the optimization problem (3.5)-(3.6) has a unique solution pair $(y, u) \in \mathcal{Y}_{\rho} \times \mathcal{U}^{ad}$ if and only if there is an adjoint $p \in \mathcal{Y}_{\rho}$ such that the following optimality system holds for the triplet (y, u, p) :

$$a[y, v]_{\rho} + b[u, v]_{\rho} = [f, v]_{\rho}, \quad v \in \mathcal{Y}_{\rho}, \quad (3.8a)$$

$$a[q, p]_{\rho} = [y - y^d, q]_{\rho} + \gamma [y - \tilde{\mathbb{E}}[y], q]_{\rho}, \quad q \in \mathcal{Y}_{\rho}, \quad (3.8b)$$

$$(\tilde{\mathbb{E}}[p] + \mu u, w - u) \geq 0, \quad w \in \mathcal{U}^{ad}. \quad (3.8c)$$

Next, we present the representation of stochastic solutions, i.e., $y(\mathbf{x}, \xi), p(\mathbf{x}, \xi)$, by using a polynomial chaos (PC) approximation [26].

3.2 Stochastic Galerkin Method

The state solution $y(\mathbf{x}, \xi) \in L^2(\Gamma, \mathcal{F}, \mathbb{P})$, as well as the adjoint solution $p(\mathbf{x}, \xi) \in L^2(\Gamma, \mathcal{F}, \mathbb{P})$, can be represented by a finite generalized polynomial chaos (PC) approximation as stated in Cameron–Martin theorem [51],

$$y(\mathbf{x}, \omega) \approx y_J(\mathbf{x}, \xi) = \sum_{i=0}^{J-1} y_i(\mathbf{x}) \psi_i(\xi), \quad (3.9a)$$

$$p(\mathbf{x}, \omega) \approx p_J(\mathbf{x}, \xi) = \sum_{i=0}^{J-1} p_i(\mathbf{x}) \psi_i(\xi), \quad (3.9b)$$

where $y_i(\mathbf{x})$ and $p_i(\mathbf{x})$ are the deterministic modes of the expansion and the total number of PC basis is determined by the dimension N of the random vector ξ and the highest order Q in the basis set of ψ_i

$$J = 1 + \sum_{s=1}^Q \frac{1}{s!} \prod_{j=0}^{s-1} (N+j) = \frac{(N+Q)!}{N!Q!}.$$

By following [49, 52], we then define the stochastic space as

$$\mathcal{S}_k := \text{span}\{\psi_i(\xi) : i = 0, 1, \dots, J-1\} \subset L^2(\Gamma). \quad (3.10)$$

For simplicity, we only deal with the state equation since the procedure for the adjoint equation is similar to the state ones. By inserting KL expansions (3.4) of the diffusion $a(\mathbf{x}, \omega)$ and the convection $\mathbf{b}(\mathbf{x}, \omega)$ coefficients, and the solution expression (3.9) into the variational form of the state equation (3.6) and projecting onto the space of the PC basis functions, we get a linear system, consisting of J deterministic convection diffusion equations for $j = 0, \dots, J-1$

$$\sum_{i=0}^{J-1} (-\nabla \cdot (a_{ij} \nabla y_i(\mathbf{x})) + \mathbf{b}_{ij} \cdot \nabla y_i(\mathbf{x})) = \langle \psi_j \rangle f(\mathbf{x}) + \langle \psi_j \rangle u(\mathbf{x}), \quad (3.11)$$

where

$$\begin{aligned} a_{ij} &= \bar{a}(\mathbf{x}) \langle \psi_i^2(\xi) \rangle \delta_{ij} + \kappa_a \sum_{k=1}^N \sqrt{\lambda_k^a} \phi_k^a(\mathbf{x}) \langle \xi_k \psi_i(\xi) \psi_j(\xi) \rangle, \\ \mathbf{b}_{ij} &= \bar{\mathbf{b}}(\mathbf{x}) \langle \psi_i^2(\xi) \rangle \delta_{ij} + \kappa_b \sum_{k=1}^N \sqrt{\lambda_k^b} \phi_k^b(\mathbf{x}) \langle \xi_k \psi_i(\xi) \psi_j(\xi) \rangle. \end{aligned}$$

Here, we apply the same distribution for both diffusion and convection random coefficients in order to reduce the computational effort. However, it can be possible to use different distributions; see, e.g. [53] for more discussion. We also note that the quantity of interest is the statistical moments of the solution $y(\mathbf{x}, \omega)$ rather than the solution $y(\mathbf{x}, \omega)$.

3.3 Symmetric interior penalty Galerkin (SIPG) method

We briefly recall the SIPG discretization following the studies in [30, 54]. A shape-regular simplicial triangulations of \mathcal{D} is denoted by $\{\mathcal{T}_h\}_h$ with $\bar{\mathcal{D}} = \bigcup_{K \in \mathcal{T}_h} \bar{K}$. The set of all edges \mathcal{E}_h consists of the interior edges \mathcal{E}_h^0 and boundary edges \mathcal{E}_h^∂ such that $\mathcal{E}_h = \mathcal{E}_h^0 \cup \mathcal{E}_h^\partial$. For a fixed realization ω and the unit outward normal \mathbf{n}_K to ∂K , we decompose the boundary edges of an element K into the inflow ∂K^-

$$\partial K^- = \{\mathbf{x} \in \partial K : \mathbf{b}(\mathbf{x}, \omega) \cdot \mathbf{n}_K(\mathbf{x}) < 0\}$$

and outflow ∂K^+ parts such that $\partial K^+ = \partial K \setminus \partial K^-$. Jump and average operators of y and ∇y for a common edge $E = K \cap K^e$ are given, respectively, by

$$[y] = y|_E \mathbf{n}_K + y^e|_E \mathbf{n}_{K^e}, \quad [\nabla y] = \nabla y|_E \cdot \mathbf{n}_K + \nabla y^e|_E \cdot \mathbf{n}_{K^e}, \quad (3.12a)$$

$$\{y\} = \frac{1}{2}(y|_E + y^e|_E), \quad \{\nabla y\} = \frac{1}{2}(\nabla y|_E + \nabla y^e|_E), \quad (3.12b)$$

where $y|_E$ (or $\nabla y|_E$) and $y^e|_E$ (or $\nabla y^e|_E$) are traces from inside K and K^e , respectively. For a boundary edge $E \in K \cap \partial \mathcal{D}$, the operators are defined by $\{\nabla y\} = \nabla y$ and $[y] = y \mathbf{n}$, where \mathbf{n} denotes the unit outward normal to $\partial \mathcal{D}$. Further, we set $h = \max_{K \in \mathcal{T}_h} h_K$, where h_K is the diameter of an element K .

Defining the discrete space as follows

$$V_h = \{y \in L^2(\mathcal{D}) : y|_K \in \mathbb{P}(K) \quad \forall K \in \mathcal{T}_h\}, \quad (3.13)$$

where $\mathbb{P}(K)$ is the set of linear polynomials and following the standard discontinuous Galerkin structure discussed in [32, 33], the (bi)-linear forms for a finite dimensional vector ξ can be stated as follow:

$$\begin{aligned} a_h(y, v, \xi) &= \sum_{K \in \mathcal{T}_h} \int_K a(., \xi) \nabla y \cdot \nabla v \, d\mathbf{x} - \sum_{E \in \mathcal{E}_h^0 \cup \mathcal{E}_h^\partial} \int_E \{a(., \xi) \nabla y\} [v] \, ds \\ &\quad - \sum_{E \in \mathcal{E}_h^0 \cup \mathcal{E}_h^\partial} \int_E \{a(., \xi) \nabla v\} [y] \, ds + \sum_{E \in \mathcal{E}_h^0 \cup \mathcal{E}_h^\partial} \frac{\sigma}{h_E} \int_E [y] \cdot [v] \, ds \\ &\quad + \sum_{K \in \mathcal{T}_h} \int_K \mathbf{b}(., \xi) \cdot \nabla y v \, d\mathbf{x} + \sum_{K \in \mathcal{T}_h} \int_{\partial K^- \setminus \partial \mathcal{D}} \mathbf{b}(., \xi) \cdot \mathbf{n}_E (y^e - y) v \, ds \\ &\quad - \sum_{K \in \mathcal{T}_h} \int_{\partial K^- \cap \partial \mathcal{D}} \mathbf{b}(., \xi) \cdot \mathbf{n}_E y v \, ds, \\ b_h(u, v, \xi) &= - \sum_{K \in \mathcal{T}_h} \int_K uv \, d\mathbf{x}, \\ l_h(f, v, \xi) &= \sum_{K \in \mathcal{T}_h} \int_K f v \, d\mathbf{x} + \sum_{E \in \mathcal{E}_h^\partial} \int_E \left(\frac{\sigma}{h_E} y_{DB} [v] - y_{DB} \{a(., \xi) \nabla v\} \right) ds \\ &\quad - \sum_{K \in \mathcal{T}_h} \int_{\partial K^- \cap \partial \mathcal{D}} \mathbf{b}(., \xi) \cdot \mathbf{n}_E y_{DB} v \, ds, \end{aligned}$$

where the parameter $\sigma \in \mathbb{R}_0^+$, called as the penalty parameter, should be sufficiently large to ensure the stability of the SIPG scheme; independent of the mesh size h . However, as discussed in [33, Sec. 2.7.1], it depends on the degree of polynomials used in the DG discretization and the position of the

edge E . In our numerical experiments, we choose σ as $\sigma = 6$ on the interior edges \mathcal{E}_h^0 and 12 on the boundary edges \mathcal{E}_h^∂ .

Then, the (bi)–linear forms of the stochastic discontinuous Galerkin (SDG) for the state equation correspond to

$$a_\xi[y, v] + b_\xi[u, v] = [f, v]_\xi,$$

where

$$\begin{aligned} a_\xi[y, v] &= \int_\Gamma a_h(y, v, \xi) \rho(\xi) d\xi, & b_\xi[u, v] &= \int_\Gamma b_h(u, v, \xi) \rho(\xi) d\xi, \\ [f, v]_\xi &= \int_\Gamma l_h(f, v, \xi) \rho(\xi) d\xi. \end{aligned}$$

Now, we can state the discrete optimal control problem

$$\begin{aligned} \min_{u_h \in \mathcal{U}_h^{ad}} \mathcal{J}(u_h) &= \frac{1}{2} \tilde{\mathbb{E}} \left[\int_{\mathcal{D}} (y_h - y^d)^2 d\mathbf{x} \right] + \frac{\gamma}{2} \tilde{\mathbb{E}} \left[\int_{\mathcal{D}} \left(y_h - \tilde{\mathbb{E}}[y_h] \right)^2 d\mathbf{x} \right] \\ &\quad + \frac{\mu}{2} \int_{\mathcal{D}} u_h^2 d\mathbf{x} \end{aligned} \quad (3.14)$$

governed by

$$a_\xi[y_h, v_h] + b_\xi[u_h, v_h] = [f, v_h]_\xi, \quad \forall v_h \in \mathcal{V}_h = V_h \otimes \mathcal{S}_k, \quad (3.15)$$

where the discrete admissible set (1.3) is defined by

$$\mathcal{U}_h^{ad} := \{u_h \in \mathcal{U}_h : u_a \leq u_h(\mathbf{x}) \leq u_b, \text{ a.e. } \mathbf{x} \in K \subset \mathcal{T}_h\}, \quad (3.16)$$

with $\mathcal{U}_h^{ad} = \mathcal{U}_h \cap \mathcal{U}^{ad}$ and $\mathcal{U}_h = \mathcal{V}_h$. Analogously, a pair $(y_h, u_h) \in \mathcal{V}_h \times \mathcal{U}_h^{ad}$ is a unique solution of the control problem (3.14)–(3.15) if and only if an adjoint $p_h \in \mathcal{Y}_h$ exists such that the optimality system holds for $(y_h, u_h, p_h) \in \mathcal{V}_h \times \mathcal{U}_h^{ad} \times \mathcal{Y}_h$

$$a_\xi[y_h, v_h] + b_\xi[u_h, v_h] = [f, v_h]_\xi, \quad v_h \in \mathcal{V}_h, \quad (3.17a)$$

$$a_\xi[q_h, p_h] = [y_h - y^d, q_h]_\xi + \gamma [y_h - \tilde{\mathbb{E}}[y_h], q_h]_\xi, \quad q_h \in \mathcal{Y}_h, \quad (3.17b)$$

$$[p_h + \mu u_h, w_h - u_h]_\xi \geq 0, \quad w_h \in \mathcal{U}_h^{ad}, \quad (3.17c)$$

where $[p_h + \mu u_h, w_h - u_h]_\xi = (\tilde{\mathbb{E}}[p_h] + \mu u_h, w_h - u_h)$ since the discrete solution u_h is deterministic.

Further, by denoting

$$\mathcal{J}'_h(u_h) \cdot w_h = [p_h + \mu u_h, w_h]_\xi, \quad \forall w_h \in \mathcal{U}_h^{ad}, \quad (3.18)$$

one can easily obtain the following expression for the discrete directional derivative of functional $\mathcal{J}_h(u_h)$:

$$\mathcal{J}'_h(u_h) \cdot (w_h - u_h) \geq 0, \quad \forall w_h \in \mathcal{U}_h^{ad}. \quad (3.19)$$

4 Error analysis

We provide an a priori error analysis of the optimization problem (2.12)–(2.13), discretized by the stochastic discontinuous Galerkin method. Before deriving the corresponding estimates, we define the associated energy norm on $\mathcal{D} \times \Gamma$ as

$$\|y\|_\xi = \left(\int_\Gamma \|y(\cdot, \xi)\|_e^2 \rho(\xi) d\xi \right)^{\frac{1}{2}}, \quad (4.1)$$

where $\|y(\cdot, \xi)\|_e$ is the energy norm on \mathcal{D} , given as

$$\begin{aligned} \|y(\cdot, \xi)\|_e = & \left(\sum_{K \in \mathcal{T}_h} \int_K a(\cdot, \xi) (\nabla y)^2 d\mathbf{x} + \sum_{E \in \mathcal{E}_h^0 \cup \mathcal{E}_h^\partial} \frac{\sigma}{h_E} \int_E \llbracket y \rrbracket^2 ds \right. \\ & \left. + \frac{1}{2} \sum_{E \in \mathcal{E}_h^\partial} \int_E \mathbf{b}(\cdot, \xi) \cdot \mathbf{n}_E y^2 ds + \frac{1}{2} \sum_{E \in \mathcal{E}_h^0} \int_E \mathbf{b}(\cdot, \xi) \cdot \mathbf{n}_E (y^e - y)^2 ds \right)^{\frac{1}{2}}. \end{aligned}$$

By the standard arguments as done in deterministic case, one can easily show the coercivity and continuity of $a_\xi(\cdot, \cdot)$ for $y, v \in \mathcal{V}_h$

$$a_\xi[y, y] \geq c_{cv} \|y\|_\xi^2, \quad a_\xi[y, v] \leq c_{ct} \|y\|_\xi \|v\|_\xi, \quad (4.2)$$

where the coercivity constant c_{cv} depends on a_{min} , whereas the continuity constant c_{ct} depends on a_{max} .

Next, we state the estimates on the finite dimensional probability domain Γ and the physical domain $K \in \mathcal{T}_h$. Let a partition of the support of probability density in finite dimensional space, i.e., $\Gamma = \prod_{n=1}^N \Gamma_n$, consists of disjoint \mathbf{R}^N –

boxes, $\gamma = \prod_{n=1}^N (r_n^\gamma, s_n^\gamma)$, with $(r_n^\gamma, s_n^\gamma) \subset \Gamma_n$ for $n = 1, \dots, N$ so that the mesh size k_n becomes $k_n = \max_\gamma |s_n^\gamma - r_n^\gamma|$, $n = 1 \dots N$. For the multi-index $q = (q_1, \dots, q_N)$, the (discontinuous) finite element approximation space having at most q_n degree on each direction ξ_n is denoted by $\mathcal{S}_k^q \subset L^2(\Gamma)$. Then, for $v \in H^{q+1}(\Gamma)$, $\varphi \in \mathcal{S}_k^q$, we have, see [43],

$$\min_{\varphi \in \mathcal{S}_k^q} \|v - \varphi\|_{L^2(\Gamma)} \leq \sum_{n=1}^N \left(\frac{k_n}{2} \right)^{q_n+1} \frac{\|\partial_{\xi_n}^{q_n+1} v\|_{L^2(\Gamma)}}{(q_n+1)!}. \quad (4.3)$$

For $v \in H^2(K)$ and $\tilde{v} \in \mathbb{P}(K)$, where $K \in \mathcal{T}_h$, the following discontinuous Galerkin approximation [33, Theorem 2.6] also holds

$$\|v - \tilde{v}\|_{H^q(K)} \leq C h^{2-q} |v|_{H^2(K)}, \quad 0 \leq q \leq 2, \quad (4.4)$$

where the constant C is not depending on v and h .

Further, we define the following projection operators, which are needed in the rest of the paper:

- L^2 -projection operators $\Pi_n : L^2(\Gamma) \rightarrow \mathcal{S}_k^q$ and $\Pi_h : L^2(\mathcal{D}) \rightarrow V_h \cap L^2(\mathcal{D})$ are given by

$$(\Pi_n(\xi) - \xi, \zeta)_{L^2(\Gamma)} = 0, \quad \forall \zeta \in \mathcal{S}_k^q, \quad \forall \xi \in L^2(\Gamma), \quad (4.5a)$$

$$(\Pi_h(\nu) - \nu, \chi)_{L^2(\mathcal{D})} = 0, \quad \forall \chi \in V_h, \quad \forall \nu \in L^2(\mathcal{D}). \quad (4.5b)$$

with the following estimate

$$\|\nu - \Pi_h(\nu)\|_{L^2(L^2(\mathcal{D}; \Gamma))} \leq Ch \|\nu\|_{L^2(H^1(\mathcal{D}; \Gamma))}. \quad (4.6)$$

In addition, taking $\zeta = \Pi_n(\xi)$ and $\chi = \Pi_h(\nu)$ in (4.5a) and (4.5b), respectively, it holds that

$$\|\Pi_n(\xi)\|_{L^2(\Gamma)} \leq C \|\xi\|_{L^2(\Gamma)}, \quad \forall \xi \in L^2(\Gamma), \quad (4.7a)$$

$$\|\Pi_h(\nu)\|_{L^2(\mathcal{D})} \leq C \|\nu\|_{L^2(\mathcal{D})}, \quad \forall \nu \in L^2(\mathcal{D}). \quad (4.7b)$$

- H^1 -projection operator $\mathcal{R}_h : H^1(\mathcal{D}) \rightarrow V_h \cap H^1(\mathcal{D})$ is stated by

$$(\mathcal{R}_h(v) - v, \vartheta)_{L^2(\mathcal{D})} = 0, \quad \forall \vartheta \in V_h, \quad \forall v \in H^1(\mathcal{D}), \quad (4.8a)$$

$$(\nabla(\mathcal{R}_h(v) - v), \nabla \vartheta)_{L^2(\mathcal{D})} = 0, \quad \forall \vartheta \in V_h, \quad \forall v \in H^1(\mathcal{D}). \quad (4.8b)$$

With the help of the H^1 -projection operator in (4.8a), the Cauchy–Schwarz inequality, the L^2 -projection operator in (4.5a), and the approximation in (4.3), we obtain the approximation property ([54, Theorem 3.2]): for all $v \in L^2(H^2(\mathcal{D}); \Gamma) \cap H^{q+1}(H^1(\mathcal{D}); \Gamma)$ and $\tilde{v} \in V_h \times \mathcal{S}_k^q$

$$\begin{aligned} \|v - \tilde{v}\|_{L^2(H^1(\mathcal{D}); \Gamma)} &\leq Ch \|v\|_{L^2(H^2(\mathcal{D}); \Gamma)} \\ &\quad + \sum_{n=1}^N \left(\frac{k_n}{2}\right)^{q_n+1} \frac{\|\partial_{\xi_n}^{q_n+1} v\|_{L^2(H^1(\mathcal{D}); \Gamma)}}{(q_n+1)!}, \end{aligned} \quad (4.9)$$

where the constant C does not depend on v , h , and k_n .

To recognize error contributions emerging from the spatial domain \mathcal{D} and the probability domain Γ , separately, a projection operator \mathcal{P}_{hn} mapping onto the tensor product space \mathcal{Y}_h is given by

$$\mathcal{P}_{hn} \Upsilon = \Pi_h \Pi_n \Upsilon = \Pi_n \Pi_h \Upsilon, \quad \forall \Upsilon \in L^2(L^2(\mathcal{D}); \Gamma) \quad (4.10)$$

and the decomposition

$$\Upsilon - \mathcal{P}_{hn}\Upsilon = (\Upsilon - \Pi_h\Upsilon) + \Pi_h(I - \Pi_n)\Upsilon, \quad \forall \Upsilon \in L^2(L^2(\mathcal{D}); \Gamma). \quad (4.11)$$

Then, it follows from (4.7a), (4.7b), and (4.10) that

$$\|\mathcal{P}_{hn}\Upsilon\|_{L^2(L^2(\mathcal{D}); \Gamma)} \leq C\|\Upsilon\|_{L^2(L^2(\mathcal{D}); \Gamma)}, \quad \forall \Upsilon \in L^2(L^2(\mathcal{D}); \Gamma). \quad (4.12)$$

Before the derivation of a priori error estimate, we state the following auxiliary problem

$$\mathcal{J}'_h(u) \cdot (w - u) = [p_h(u) + \mu u, w - u]_\xi \geq 0, \quad \forall w \in \mathcal{U}^{ad}, \quad (4.13)$$

where $p_h(u) \in \mathcal{Y}_h$ solves the following auxiliary system:

$$a_\xi[y_h(u), v_h] + b_\xi[u, v_h] = [f, v_h]_\xi, \quad v_h \in \mathcal{Y}_h, \quad (4.14a)$$

$$a_\xi[q_h, p_h(u)] = [y_h(u) - y^d, q_h]_\xi + \gamma[y_h(u) - \tilde{\mathbb{E}}[y_h(u)], q_h]_\xi, \quad q_h \in \mathcal{Y}_h. \quad (4.14b)$$

It is also noted that we prefer to use $\|u\|_{L^2(L^2(\mathcal{D}); \Gamma)}$ in the derivation of error estimates instead of $\|u\|_{L^2(\mathcal{D})}$ for better readability in terms of notation.

Lemma 4.1. *With the definition in (4.13), the following estimate holds:*

$$(\mathcal{J}'_h(w) - \mathcal{J}'_h(u)) \cdot (w - u) \geq \mu\|w - u\|_{L^2(L^2(\mathcal{D}); \Gamma)}^2. \quad (4.15)$$

Proof By (4.13), we have

$$(\mathcal{J}'_h(w) - \mathcal{J}'_h(u)) \cdot (w - u) = [p_h(w) - p_h(u), w - u]_\xi + \mu[w - u, w - u]_\xi. \quad (4.16)$$

Now, it follows from (4.14) that

$$\begin{aligned} [p_h(w) - p_h(u), w - u]_\xi &= a_\xi[y_h(w) - y_h(u), p_h(w) - p_h(u)] \\ &= (1 + \gamma)[y_h(w) - y_h(u), y_h(w) - y_h(u)]_\xi \\ &\quad - \gamma[\tilde{\mathbb{E}}[y_h(w) - y_h(u)], y_h(w) - y_h(u)]_\xi. \end{aligned} \quad (4.17)$$

The usage of Cauchy-Schwarz and Young's inequalities yields

$$\begin{aligned} & -\gamma[\tilde{\mathbb{E}}[y_h(w) - y_h(u)], y_h(w) - y_h(u)]_\xi \\ & \geq -\frac{\gamma}{2}\|\tilde{\mathbb{E}}[y_h(w) - y_h(u)]\|_{L^2(L^2(\mathcal{D}); \Gamma)}^2 - \frac{\gamma}{2}\|y_h(w) - y_h(u)\|_{L^2(L^2(\mathcal{D}); \Gamma)}^2. \end{aligned}$$

Since all norms are convex functions, Jensen's inequality $\|\tilde{\mathbb{E}}[u]\| \leq \tilde{\mathbb{E}}\|u\|$ and $\tilde{\mathbb{E}}[\tilde{\mathbb{E}}[u]] = \tilde{\mathbb{E}}[u]$ give us

$$-\gamma[\tilde{\mathbb{E}}[y_h(w) - y_h(u)], y_h(w) - y_h(u)]_\xi \geq -\gamma\|y_h(w) - y_h(u)\|_{L^2(L^2(\mathcal{D}); \Gamma)}^2. \quad (4.18)$$

Thus, inserting (4.18) into (4.17), it is obtained that

$$[p_h(w) - p_h(u), w - u]_\xi \geq \underbrace{\|y_h(w) - y_h(u)\|_{L^2(L^2(\mathcal{D}); \Gamma)}^2}_{\geq 0}. \quad (4.19)$$

Hence, (4.16) and (4.19) imply that (4.15) holds. \square

Next, we derive an upper bound for the error between the discrete solutions (y_h, p_h) and the auxiliary solutions $(y_h(u), p_h(u))$.

Lemma 4.2. *Assume that (y_h, p_h) and $(y_h(u), p_h(u))$, respectively, are the solutions of (3.17) and (4.14). Then, the following estimates exist for positive constants C_1 and C_2 independent of h*

$$\|y_h - y_h(u)\|_\xi \leq C_1 \|u - u_h\|_{L^2(L^2(\mathcal{D}); \Gamma)}, \quad (4.20a)$$

$$\|p_h - p_h(u)\|_\xi \leq C_2 \|u - u_h\|_{L^2(L^2(\mathcal{D}); \Gamma)}. \quad (4.20b)$$

Proof By subtracting (4.14a) from (3.17a) and taking $v_h = y_h - y_h(u)$, we have that

$$a_\xi[y_h - y_h(u), y_h - y_h(u)] = [u_h - u, y_h - y_h(u)]_\xi.$$

With the help of the coercivity of a_ξ (4.2) and the Cauchy-Schwarz inequality, we obtain

$$\begin{aligned} c_{cv} \|y_h - y_h(u)\|_\xi^2 &\leq a_\xi[y_h - y_h(u), y_h - y_h(u)] \\ &\leq \|u_h - u\|_{L^2(L^2(\mathcal{D}); \Gamma)} \|y_h - y_h(u)\|_\xi, \end{aligned}$$

which yields the desired result (4.20a).

Analogously, by subtracting (4.14b) from (3.17b) and taking $v_h = p_h - p_h(u)$, we have that

$$\begin{aligned} a_\xi[p_h - p_h(u), p_h - p_h(u)] \\ = (1 + \gamma)[y_h - y_h(u), p_h - p_h(u)]_\xi + \gamma \left[\tilde{\mathbb{E}}[y_h(u) - y_h], p_h - p_h(u) \right]_\xi. \end{aligned}$$

It follows from the coercivity of a_ξ , Cauchy-Schwarz inequality, and Jensen's inequality that

$$\begin{aligned} c_{cv} \|p_h - p_h(u)\|_\xi^2 &\leq a_\xi[p_h - p_h(u), p_h - p_h(u)] \\ &\leq (1 + 2\gamma) \|p_h - p_h(u)\|_{L^2(L^2(\mathcal{D}); \Gamma)} \|y_h - y_h(u)\|_\xi. \end{aligned} \quad (4.21)$$

We note that the procedure applied in (4.18) is also used in the derivation of (4.21). Hence, by (4.21) and (4.20a), we deduce the desired result (4.20b). \square

To obtain an upper bound for the control, we divide the domain \mathcal{D} into pieces by considering the active and inactive parts of the control u as done in [55, 56]:

$$\mathcal{D}^+ = \left\{ \bigcup_K : K \subset \mathcal{D}, u_a < u|_K < u_b \right\}, \quad (4.22a)$$

$$\mathcal{D}^\partial = \left\{ \bigcup_K : K \subset \mathcal{D}, u|_K = u_a \text{ or } u|_K = u_b \right\}, \quad (4.22b)$$

$$\mathcal{D}^- = \mathcal{D} \setminus (\mathcal{D}^+ \cup \mathcal{D}^\partial). \quad (4.22c)$$

It is assumed that these sets are disjoint, $\mathcal{D} = \mathcal{D}^+ \cup \mathcal{D}^\partial \cup \mathcal{D}^-$, and \mathcal{D}^- satisfies the following inequality related to the regularity of u and \mathcal{T}_h

$$\text{meas}(\mathcal{D}^-) \leq Ch, \quad (4.23)$$

which is valid if the boundary of the \mathcal{D}^∂ is represented by finite rectifiable curves [57]. Further, we define a set such that $\mathcal{D}^+ \subset \mathcal{D}^* = \{\mathbf{x} \in \mathcal{D} : u_a < u(\mathbf{x}) < u_b\}$ [58].

Lemma 4.3. *Let (y, u, p) and (y_h, u_h, p_h) , respectively, be the solutions of (2.15) and (3.17). Assume that $u \in L^2(W^{1,\infty}(\mathcal{D}); \Gamma)$ with $u|_{\mathcal{D}^+} \in L^2(H^2(\mathcal{D}^+); \Gamma)$. Then, it holds that*

$$\begin{aligned} & \|u - u_h\|_{L^2(L^2(\mathcal{D}); \Gamma)} \\ & \leq C\|p - p_h(u)\|_{L^2(L^2(\mathcal{D}; \Gamma))} + Ch^{3/2}\|u\|_{L^2(W^{1,\infty}(\mathcal{D}); \Gamma)} \\ & \quad + C\left(h\|p\|_{L^2(H^1(\mathcal{D}); \Gamma)} + \sum_{n=1}^N \left(\frac{k_n}{2}\right)^{q_n+1} \frac{\|\partial_{\xi_n}^{q_n+1} p\|_{L^2(H^1(\mathcal{D}; \Gamma))}}{(q_n+1)!}\right). \end{aligned} \quad (4.24)$$

Proof With the help of Lemma 4.1, (4.13), the standard Lagrangian interpolation Πu , the assumption $\mathcal{D}^+ \subset \mathcal{D}^*$, and the notation $p_h = p_h(u_h)$, we obtain

$$\begin{aligned} \mu\|u - u_h\|_{L^2(L^2(\mathcal{D}); \Gamma)}^2 & \leq \mathcal{J}'_h(u) \cdot (u - u_h) - \mathcal{J}'_h(u_h) \cdot (u - u_h) \\ & = [\mu u + p_h(u), u - u_h]_\xi - [\mu u_h + p_h, u - u_h]_\xi \\ & = [\mu u + p, u - u_h]_\xi - [p - p_h(u), u - u_h]_\xi \\ & \quad - \underbrace{\mathcal{J}'(u) \cdot (u_h - u)}_{\leq 0} \\ & \quad + [\mu u_h + p_h, u_h - \Pi u]_\xi + [\mu u_h + p_h, \Pi u - u]_\xi \\ & \quad - \underbrace{\mathcal{J}'_h(u_h) \cdot (\Pi u - u_h)}_{\leq 0} \\ & \leq [\mu u_h + p_h, \Pi u - u]_\xi + [p_h(u) - p, u - u_h]_\xi. \end{aligned} \quad (4.25)$$

The first term in (4.25) can be rewritten as follows

$$\begin{aligned} [\mu u_h + p_h, \Pi u - u]_\xi & = [\mu u_h + p_h - \mu u - p, \Pi u - u]_\xi + [\mu u + p, \Pi u - u]_\xi \\ & = [\mu u_h - \mu u, \Pi u - u]_\xi + [\mu u + p, \Pi u - u]_\xi \\ & \quad + [p_h - p_h(u), \Pi u - u]_\xi + [p_h(u) - p, \Pi u - u]_\xi. \end{aligned} \quad (4.26)$$

Then, inserting (4.26) into (4.25) and applying Cauchy-Schwarz and Young's inequalities and Lemma 4.2, we obtain

$$\begin{aligned} \mu\|u - u_h\|_{L^2(L^2(\mathcal{D}); \Gamma)}^2 & \leq c_1\|p_h(u) - p\|_{L^2(L^2(\mathcal{D}); \Gamma)}^2 + c_2\|u - u_h\|_{L^2(L^2(\mathcal{D}); \Gamma)}^2 \\ & \quad + c_3\|u - \Pi u\|_{L^2(L^2(\mathcal{D}); \Gamma)}^2 + [\mu u + p, \Pi u - u]_\xi. \end{aligned} \quad (4.27)$$

Since $\Pi u(\mathbf{x}) = u(\mathbf{x})$ for any vertex \mathbf{x} , $\Pi u \in \mathcal{U}_h^{ad}$ and the following estimates hold

$$\|u - \Pi u\|_{L^2(L^2(\mathcal{D}^+); \Gamma)} \leq Ch^2\|u\|_{L^2(H^2(\mathcal{D}^+); \Gamma)}, \quad (4.28a)$$

$$\|u - \Pi u\|_{L^2(W^{0,\infty}(\mathcal{D}^-); \Gamma)} \leq Ch\|u\|_{L^2(W^{1,\infty}(\mathcal{D}^-); \Gamma)} \quad (4.28b)$$

for $u \in L^2(W^{1,\infty}(\mathcal{D}); \Gamma)$ and $u|_{\mathcal{D}^*} \in L^2(H^2(\mathcal{D}^*); \Gamma)$. Hence

$$\begin{aligned} & \|u - \Pi u\|_{L^2(L^2(\mathcal{D}); \Gamma)}^2 \\ & = \|u - \Pi u\|_{L^2(L^2(\mathcal{D}^+); \Gamma)}^2 + \underbrace{\|u - \Pi u\|_{L^2(L^2(\mathcal{D}^\partial); \Gamma)}^2}_{=0} + \|u - \Pi u\|_{L^2(L^2(\mathcal{D}^-); \Gamma)}^2 \end{aligned}$$

$$\begin{aligned}
&\leq \|u - \Pi u\|_{L^2(L^2(\mathcal{D}^+); \Gamma)}^2 + C\|u - \Pi u\|_{L^2(W^{0,\infty}(\mathcal{D}^-); \Gamma)}^2 \text{meas}(\mathcal{D}^-) \\
&\leq Ch^4 \|u\|_{L^2(H^2(\mathcal{D}^+); \Gamma)}^2 + Ch^3 \|u\|_{L^2(W^{1,\infty}(\mathcal{D}^-); \Gamma)}^2 \\
&\leq Ch^3 \left(h\|u\|_{L^2(H^2(\mathcal{D}^+); \Gamma)}^2 + \|u\|_{L^2(W^{1,\infty}(\mathcal{D}^-); \Gamma)}^2 \right) \\
&\leq Ch^3 \left(\|u\|_{L^2(H^2(\mathcal{D}^+); \Gamma)}^2 + \|u\|_{L^2(W^{1,\infty}(\mathcal{D}^-); \Gamma)}^2 \right). \tag{4.29}
\end{aligned}$$

By the variational inequality (3.17c) and the definitions of domains (4.22), we have

$$\mu u + p = 0 \text{ on } \mathcal{D}^+ \quad \text{and} \quad \Pi u - u = 0 \text{ on } \mathcal{D}^\partial.$$

Then,

$$\begin{aligned}
[\mu u + p, \Pi u - u]_\xi &= \underbrace{[\mu u - \Pi_h(\mu u) + \Pi_h(\mu u), \Pi u - u]_{\mathcal{D}^-}}_{T_1} \\
&\quad + \underbrace{[p - \mathcal{P}_{hn}(p) + \mathcal{P}_{hn}(p), \Pi u - u]_{\mathcal{D}^-}}_{T_2}. \tag{4.30}
\end{aligned}$$

It follows from the inequalities (4.6), (4.7b), and (4.28b), Sobolev embedding theorem, see, e.g., [59], and Young's inequality that

$$\begin{aligned}
T_1 &= [\mu u - \Pi_h(\mu u), \Pi u - u]_{\mathcal{D}^-} + [\Pi_h(\mu u), \Pi u - u]_{\mathcal{D}^-} \\
&\leq \mu \left(\|u - \Pi_h u\|_{L^2(L^2(\mathcal{D}^-); \Gamma)} + \|\Pi_h u\|_{L^2(L^2(\mathcal{D}^-); \Gamma)} \right) \|u - \Pi u\|_{L^2(L^2(\mathcal{D}^-); \Gamma)} \\
&\leq \mu \left(\|u - \Pi_h u\|_{L^2(L^2(\mathcal{D}^-); \Gamma)} + C\|u\|_{L^2(L^2(\mathcal{D}^-); \Gamma)} \right) \|u - \Pi u\|_{L^2(L^2(\mathcal{D}^-); \Gamma)} \\
&\leq \mu \left(\|u - \Pi_h u\|_{L^2(L^2(\mathcal{D}^-); \Gamma)} + C\|u\|_{L^2(W^{0,\infty}(\mathcal{D}^-); \Gamma)} \text{meas}(\mathcal{D}^-) \right) \\
&\quad \times \|u - \Pi u\|_{L^2(L^2(\mathcal{D}^-); \Gamma)} \\
&\leq Ch\|u\|_{L^2(H^1(\mathcal{D}^-); \Gamma)} \|u - \Pi u\|_{L^2(W^{0,\infty}(\mathcal{D}^-); \Gamma)} \text{meas}(\mathcal{D}^-) \\
&\leq Ch^3 \|u\|_{L^2(H^1(\mathcal{D}^-); \Gamma)} \|u\|_{L^2(W^{1,\infty}(\mathcal{D}^-); \Gamma)} \\
&\leq Ch^3 \left(\|u\|_{L^2(H^1(\mathcal{D}^-); \Gamma)}^2 + \|u\|_{L^2(W^{1,\infty}(\mathcal{D}^-); \Gamma)}^2 \right). \tag{4.31}
\end{aligned}$$

Next, with the help of the projector operator in (4.10) and the bounds in (4.3), (4.6), (4.12), and (4.28b), Sobolev embedding theorem, and Cauchy and Young's inequalities, we find a bound for the second term T_2 in (4.30)

$$\begin{aligned}
T_2 &= [p - \Pi_h(p), \Pi u - u]_{\mathcal{D}^-} + [\mathcal{P}_{hn}(p), \Pi u - u]_{\mathcal{D}^-} + [\Pi_h(I - \Pi_n)(p), \Pi u - u]_{\mathcal{D}^-} \\
&\leq \left(\|p - \Pi_h(p)\|_{L^2(L^2(\mathcal{D}^-); \Gamma)} + \|\mathcal{P}_{hn}(p)\|_{L^2(L^2(\mathcal{D}^-); \Gamma)} \right) \|\Pi u - u\|_{L^2(L^2(\mathcal{D}^-); \Gamma)} \\
&\quad + \|\Pi_h(I - \Pi_n)(p)\|_{L^2(L^2(\mathcal{D}^-); \Gamma)} \|\Pi u - u\|_{L^2(L^2(\mathcal{D}^-); \Gamma)} \\
&\leq C_1 \left(h\|p\|_{L^2(H^1(\mathcal{D}^-); \Gamma)} + \|p\|_{L^2(W^{0,\infty}(\mathcal{D}^-); \Gamma)} \text{meas}(\mathcal{D}^-) \right) h^2 \|u\|_{L^2(W^{1,\infty}(\mathcal{D}^-); \Gamma)} \\
&\quad + C_2 \sum_{n=1}^N \left(\frac{k_n}{2} \right)^{q_n+1} \frac{\|\partial_{\xi_n}^{q_n+1} p\|_{L^2(H^1(\mathcal{D}^-); \Gamma)}}{(q_n+1)!} h^2 \|u\|_{L^2(W^{1,\infty}(\mathcal{D}^-); \Gamma)} \\
&\leq C_1 \left(\frac{h^2}{2} \|p\|_{L^2(H^1(\mathcal{D}^-); \Gamma)}^2 + \frac{h^4}{2} \|u\|_{L^2(W^{1,\infty}(\mathcal{D}^-); \Gamma)}^2 \right) \\
&\quad + C_2 \left(\frac{1}{2} \sum_{n=1}^N \left(\frac{k_n}{2} \right)^{2q_n+2} \frac{\|\partial_{\xi_n}^{q_n+1} p\|_{L^2(H^1(\mathcal{D}^-); \Gamma)}^2}{((q_n+1)!)^2} + \frac{h^4}{2} \|u\|_{L^2(W^{1,\infty}(\mathcal{D}^-); \Gamma)}^2 \right). \tag{4.32}
\end{aligned}$$

Combination of (4.31) and (4.32) yields

$$\begin{aligned} & [\mu u + p, \Pi u - u]_{\xi} \\ & \leq Ch^3 \left(\|u\|_{L^2(H^1(\mathcal{D}^-); \Gamma)}^2 + \|u\|_{L^2(W^{1,\infty}(\mathcal{D}^-); \Gamma)}^2 \right) \\ & \quad + Ch^2 \|p\|_{L^2(H^1(\mathcal{D}^-); \Gamma)}^2 + C \sum_{n=1}^N \left(\frac{k_n}{2} \right)^{2q_n+2} \frac{\|\partial_{\xi_n}^{q_n+1} p\|_{L^2(H^1(\mathcal{D}^-); \Gamma)}^2}{((q_n+1)!)^2}. \end{aligned} \quad (4.33)$$

Finally, inserting (4.29) and (4.33) into (4.27), we completes the proof of Lemma 4.3. \square

Lemma 4.4. *Assume that (y, p) and $(y_h(u), p_h(u))$, respectively, are the solutions of (2.15) and (4.14). Then, we have*

$$\begin{aligned} \|y - y_h(u)\|_{\xi} & \leq Ch \|y\|_{L^2(H^2(\mathcal{D}); \Gamma)} \\ & \quad + \sum_{n=1}^N \left(\frac{k_n}{2} \right)^{q_n+1} \frac{\|\partial_{\xi_n}^{q_n+1} y\|_{L^2(H^1(\mathcal{D}); \Gamma)}}{(q_n+1)!} \end{aligned} \quad (4.34)$$

and

$$\begin{aligned} & \|p - p_h(u)\|_{\xi} \\ & \leq Ch \left(\|y\|_{L^2(H^2(\mathcal{D}); \Gamma)} + \|p\|_{L^2(H^2(\mathcal{D}); \Gamma)} \right) \\ & \quad + \sum_{n=1}^N \left(\frac{k_n}{2} \right)^{q_n+1} \frac{\left(\|\partial_{\xi_n}^{q_n+1} y\|_{L^2(H^1(\mathcal{D}); \Gamma)} + \|\partial_{\xi_n}^{q_n+1} p\|_{L^2(H^1(\mathcal{D}); \Gamma)} \right)}{(q_n+1)!}. \end{aligned} \quad (4.35)$$

Proof An application of the coercivity and continuity of a_{ξ} in (4.2), $H^1(\mathcal{D})$ -projection \mathcal{R}_h in (4.8), $L^2(\mathcal{D})$ -projection Π_n in (4.5a), and Galerkin orthogonality yields

$$\begin{aligned} & c_{cv} \|y - y_h(u)\|_{\xi}^2 \\ & \leq a_{\xi}[y - y_h(u), y - y_h(u)] \\ & \leq a_{\xi}[y - y_h(u), y - \Pi_n(\mathcal{R}_h(y))] + \underbrace{a_{\xi}[y - y_h(u), \Pi_n(\mathcal{R}_h(y)) - y_h(u)]}_{=0} \\ & \leq c_{ct} \|y - y_h(u)\|_{\xi} \|y - \Pi_n(\mathcal{R}_h(y))\|_{\xi}. \end{aligned}$$

Then, by the approximation property (4.9), we get

$$\begin{aligned} \|y - y_h(u)\|_{\xi} & \leq \frac{c_{ct}}{c_{cv}} \|y - \Pi_n(\mathcal{R}_h(y))\|_{\xi} \\ & \leq Ch \|y\|_{L^2(H^2(\mathcal{D}); \Gamma)} + \sum_{n=1}^N \left(\frac{k_n}{2} \right)^{q_n+1} \frac{\|\partial_{\xi_n}^{q_n+1} y\|_{L^2(H^1(\mathcal{D}); \Gamma)}}{(q_n+1)!}, \end{aligned}$$

which is the desired result (4.34). Analogously, we deduce that

$$c_{cv} \|p - p_h(u)\|_{\xi}^2$$

$$\begin{aligned}
&\leq a_\xi[p - p_h(u), p - p_h(u)] \\
&\leq a_\xi[p - \Pi_n(\mathcal{R}_h(y)), p - p_h(u)] + \underbrace{a_\xi[\Pi_n(\mathcal{R}_h(y)) - p_h(u), p - p_h(u)]}_{=0} \\
&= (1 + \gamma)[y - y_h(u), p - \Pi_n(\mathcal{R}_h(y))]_\xi + \gamma[\tilde{\mathbb{E}}[y_h(u) - y], p - \Pi_n(\mathcal{R}_h(y))]_\xi \\
&\leq (1 + 2\gamma)\|y - y_h(u)\|_\xi \|p - \Pi_n(\mathcal{R}_h(y))\|_{L^2(L^2(\mathcal{D}); \Gamma)} \\
&\leq \frac{(1 + 2\gamma)}{2}\|y - y_h(u)\|_\xi^2 + \frac{(1 + 2\gamma)}{2}\|p - \Pi_n(\mathcal{R}_h(y))\|_{L^2(L^2(\mathcal{D}); \Gamma)}^2,
\end{aligned}$$

where the definition of bilinear forms, the procedure applied in (4.18), and Young's inequality are used. Then, using the approximation property (4.9) and (4.34), we complete the proof of (4.35). \square

Now, we finalize the error analysis by combining the findings in Lemmas 4.3 and 4.4.

Theorem 4.5. *Assume that (y, u, p) and (y_h, u_h, p_h) , respectively, are the solutions of (2.15) and (3.17). Then, it holds that*

$$\begin{aligned}
&\|u - u_h\|_{L^2(L^2(\mathcal{D}); \Gamma)} + \|y - y_h\|_\xi + \|p - p_h\|_\xi \\
&\leq Ch^{3/2}\|u\|_{L^2(W^{1,\infty}(\mathcal{D}); \Gamma)} + Ch(\|y\|_{L^2(H^2(\mathcal{D}); \Gamma)} + \|p\|_{L^2(H^2(\mathcal{D}); \Gamma)}) \\
&\quad + C \sum_{n=1}^N \left(\frac{k_n}{2}\right)^{q_n+1} \frac{\left(\|\partial_{\xi_n}^{q_n+1} y\|_{L^2(H^1(\mathcal{D}); \Gamma)} + \|\partial_{\xi_n}^{q_n+1} p\|_{L^2(H^1(\mathcal{D}); \Gamma)}\right)}{(q_n + 1)!}. \quad (4.36)
\end{aligned}$$

Proof From (4.24) and (4.35), we obtain that

$$\begin{aligned}
&\|u - u_h\|_{L^2(L^2(\mathcal{D}); \Gamma)} \\
&\leq Ch^{3/2}\|u\|_{L^2(W^{1,\infty}(\mathcal{D}); \Gamma)} + Ch(\|y\|_{L^2(H^2(\mathcal{D}); \Gamma)} + \|p\|_{L^2(H^2(\mathcal{D}); \Gamma)}) \\
&\quad + C \sum_{n=1}^N \left(\frac{k_n}{2}\right)^{q_n+1} \frac{\left(\|\partial_{\xi_n}^{q_n+1} y\|_{L^2(H^1(\mathcal{D}); \Gamma)} + \|\partial_{\xi_n}^{q_n+1} p\|_{L^2(H^1(\mathcal{D}); \Gamma)}\right)}{(q_n + 1)!}. \quad (4.37)
\end{aligned}$$

Moreover, by Lemmas 4.2 and 4.4, and the bound (4.37), we obtain

$$\begin{aligned}
&\|y - y_h\|_\xi + \|p - p_h\|_\xi \\
&\leq \|y - y_h(u)\|_\xi + \|y_h(u) - y_h\|_\xi + \|p - p_h(u)\|_\xi + \|p_h(u) - p_h\|_\xi \\
&\leq C\|u - u_h\|_{L^2(L^2(\mathcal{D}); \Gamma)} + Ch(\|y\|_{L^2(H^2(\mathcal{D}); \Gamma)} + \|p\|_{L^2(H^2(\mathcal{D}); \Gamma)}) \\
&\quad + C \sum_{n=1}^N \left(\frac{k_n}{2}\right)^{q_n+1} \left(\frac{\|\partial_{\xi_n}^{q_n+1} y\|_{L^2(H^1(\mathcal{D}); \Gamma)} + \|\partial_{\xi_n}^{q_n+1} p\|_{L^2(H^1(\mathcal{D}); \Gamma)}}{(q_n + 1)!}\right). \quad (4.38)
\end{aligned}$$

Thus, by combining (4.37) and (4.38), we deduce the desired result (4.36). \square

5 Matrix Formulation

In this section, we first construct the matrix formulation of the underlying problem (2.12)–(2.13) by employing the “optimize-then-discretize” approach;

see, e.g., [42]. In this methodology, one first obtains the optimality system (2.15) of the infinite-dimensional optimization problem, and then discretizes the optimality system by a stochastic discontinuous Galerkin method discussed in Section 3. Later, we propose a low-rank variant of generalized minimal residual (GMRES) method with a suitable preconditioner to solve the corresponding linear system.

5.1 State system

After an application of the discretization techniques discussed in Section 3, one gets the following linear system for the state part of the optimality system (2.15):

$$\underbrace{\left(\sum_{i=0}^N \mathcal{G}_i \otimes \mathcal{K}_i \right)}_{\mathcal{A}} \mathbf{y} - \underbrace{(\mathcal{G}_0 \otimes M)}_{\mathcal{M}} \mathbf{u} = \underbrace{\left(\sum_{i=0}^N \mathbf{g}_i \otimes \mathbf{f}_i \right)}_{\mathcal{F}}, \quad (5.1)$$

where $\mathbf{y} = (y_0, \dots, y_{J-1})^T$ and $\mathbf{u} = (u_0, \dots, u_{J-1})^T$ with $y_i, u_i \in \mathbb{R}^{N_d}$, $i = 0, 1, \dots, J-1$ and N_d corresponds to the degree of freedom for the spatial discretization. The mass matrix $M \in \mathbb{R}^{N_d \times N_d}$, the stiffness matrices $\mathcal{K}_i \in \mathbb{R}^{N_d \times N_d}$, and the right-hand side vectors $\mathbf{f}_i \in \mathbb{R}^{N_d}$ are given, respectively, by

$$\begin{aligned} M(r, s) &= \sum_{K \in \mathcal{T}_h} \int_K \varphi_r \varphi_s \, d\mathbf{x}, \\ \mathcal{K}_0(r, s) &= \sum_{K \in \mathcal{T}_h} \int_K (\bar{\mathbf{a}} \nabla \varphi_r \cdot \nabla \varphi_s + \bar{\mathbf{b}} \cdot \nabla \varphi_r \varphi_s) \, d\mathbf{x} \\ &\quad - \sum_{E \in \mathcal{E}_h^0 \cup \mathcal{E}_h^\partial} \int_E (\{\{\bar{\mathbf{a}} \nabla \varphi_r\}\} [\varphi_s] + \{\{\bar{\mathbf{a}} \nabla \varphi_s\}\} [\varphi_r]) \, ds \\ &\quad + \sum_{E \in \mathcal{E}_h^0 \cup \mathcal{E}_h^\partial} \frac{\sigma}{h_E} \int_E [\varphi_r] \cdot [\varphi_s] \, ds + \sum_{K \in \mathcal{T}_h} \int_{\partial K^- \setminus \partial \mathcal{D}} \bar{\mathbf{b}} \cdot \mathbf{n}_E (\varphi_r^e - \varphi_r) \varphi_s \, ds \\ &\quad - \sum_{K \in \mathcal{T}_h} \int_{\partial K^- \cap \partial \mathcal{D}^-} \bar{\mathbf{b}} \cdot \mathbf{n}_E \varphi_r \varphi_s \, ds, \\ \mathcal{K}_i(r, s) &= \sum_{K \in \mathcal{T}_h} \int_K \left((\kappa_a \sqrt{\lambda_i^a} \phi_i^a) \nabla \varphi_r \cdot \nabla \varphi_s + (\kappa_b \sqrt{\lambda_i^b} \phi_i^b) \cdot \nabla \varphi_r \varphi_s \right) \, d\mathbf{x} \\ &\quad - \sum_{E \in \mathcal{E}_h^0 \cup \mathcal{E}_h^\partial} \int_E \left(\{\{\kappa_a \sqrt{\lambda_i^a} \phi_i^a\} \nabla \varphi_r\}\} [\varphi_s] + \{\{\kappa_a \sqrt{\lambda_i^a} \phi_i^a\} \nabla \varphi_s\}\} [\varphi_r] \right) \, ds \\ &\quad + \sum_{E \in \mathcal{E}_h^0 \cup \mathcal{E}_h^\partial} \frac{\sigma}{h_E} \int_E [\varphi_r] \cdot [\varphi_s] \, ds \end{aligned}$$

$$\begin{aligned}
& + \sum_{K \in \mathcal{T}_h} \int_{\partial K^- \setminus \partial \mathcal{D}} \left(\kappa_{\mathbf{b}} \sqrt{\lambda_i^{\mathbf{b}}} \phi_i^{\mathbf{b}} \right) \cdot \mathbf{n}_E (\varphi_r^e - \varphi_r) \varphi_s \, ds \\
& - \sum_{T \in \mathcal{T}_h} \int_{\partial T^- \cap \partial \mathcal{D}^-} \left(\kappa_{\mathbf{b}} \sqrt{\lambda_i^{\mathbf{b}}} \phi_i^{\mathbf{b}} \right) \cdot \mathbf{n}_E \varphi_r \varphi_s \, ds, \\
f_0(s) &= \sum_{K \in \mathcal{T}_h} \int_K f \varphi_s \, d\mathbf{x} + \sum_{E \in \mathcal{E}_h^\partial} \frac{\sigma}{h_E} \int_E y_{DB} [\varphi_s] \, ds - \sum_{E \in \mathcal{E}_h^\partial} \int_E y_{DB} \{ \bar{a} \nabla \varphi_s \} \, ds \\
& - \sum_{K \in \mathcal{T}_h} \int_{\partial K^- \cap \partial \mathcal{D}^-} \bar{\mathbf{b}} \cdot \mathbf{n}_E y_{DB} \varphi_s \, ds, \\
f_i(s) &= \sum_{E \in \mathcal{E}_h^\partial} \frac{\sigma}{h_E} \int_E y_{DB} [\varphi_s] \, ds - \sum_{E \in \mathcal{E}_h^\partial} \int_E y_{DB} \left\{ \left(\kappa_a \sqrt{\lambda_i^a} \phi_i^a \right) \nabla \varphi_s \right\} \, ds \\
& - \sum_{K \in \mathcal{T}_h} \int_{\partial K^- \cap \partial \mathcal{D}^-} \left(\kappa_{\mathbf{b}} \sqrt{\lambda_i^{\mathbf{b}}} \phi_i^{\mathbf{b}} \right) \cdot \mathbf{n}_E y_{DB} \varphi_s \, ds,
\end{aligned}$$

where $\{\varphi_i(\mathbf{x})\}$ corresponds to the set of basis functions for the spatial discretization, i.e., $V_h = \text{span}\{\varphi_i(\mathbf{x})\}$.

On the other hand, for $i = 0, \dots, N$, the stochastic matrices $\mathcal{G}_i \in \mathbb{R}^{J \times J}$ and the stochastic vectors $\mathbf{g}_i \in \mathbb{R}^J$ in (5.1) are given, respectively, by

$$\mathcal{G}_0(r, s) = \langle \psi_r, \psi_s \rangle, \quad \mathcal{G}_i(r, s) = \langle \xi_i \psi_r, \psi_s \rangle, \quad (5.2a)$$

$$\mathbf{g}_0(r) = \langle \psi_r \rangle, \quad \mathbf{g}_i(r) = \langle \xi_i \psi_r \rangle. \quad (5.2b)$$

In (5.2), each stochastic basis function $\psi_i(\xi)$ is a product of N univariate orthogonal polynomials, i.e., $\psi_i(\xi) = \psi_{i_1}(\xi) \psi_{i_2}(\xi) \dots \psi_{i_N}(\xi)$, where the multi-index i is defined by $i = (i_1, i_2, \dots, i_N)$ with $\sum_{s=1}^N i_s \leq Q$. In this paper, Legendre polynomials are chosen as the stochastic basis functions since the underlying random variables have uniform distribution on $[-\sqrt{3}, \sqrt{3}]$ [54]. Then, \mathcal{G}_0 becomes an identity matrix, whereas \mathcal{G}_k , $k > 0$, contains at most two nonzero entries per row; see, e.g., [49, 52]. On the other hand, \mathbf{g}_i is the first column of \mathcal{G}_i , $i = 0, 1, \dots, N$.

5.2 Matrix formulation of the optimality system

The discrete optimality system in (3.17) can be represented as a block matrix system including the state, adjoint, and variational equations in the finite dimensional setting. To solve the underlying block linear system, “the primal-dual active set (PDAS) methodology as a semi-smooth Newton step” is applied; see, e.g., [60] for more details. After a definition of the active sets

$$A^- = \bigcup \{ \mathbf{x} \in K : -\mathbf{p} - \mu \mathbf{u}_a < 0, \forall K \in \mathcal{T}_h \},$$

$$A^+ = \bigcup \{ \mathbf{x} \in K : -\mathbf{p} - \mu \mathbf{u}_b > 0, \forall K \in \mathcal{T}_h \},$$

and the inactive set

$$\mathcal{I} = \mathcal{T}_h \setminus (A^- \cup A^+),$$

the block formulation becomes

$$\mathcal{A} \mathbf{y} - \mathcal{M}_I \mathbf{u} = \mathcal{F}, \quad (5.3a)$$

$$\mathcal{A}^* \mathbf{p} - \mathcal{M}_\gamma \mathbf{y} = -\mathcal{F}^d, \quad (5.3b)$$

$$(\mathcal{G}_0 \otimes \text{diag}(\mathbb{1}_{\mathcal{I}})) \mathbf{p} + \mu (\mathcal{G}_0 \otimes I) \mathbf{u} = (\mathbf{g}_0 \otimes \mathbb{1}_{A^-}) \mu \mathbf{u}_a + (\mathbf{g}_0 \otimes \mathbb{1}_{A^+}) \mu \mathbf{u}_b, \quad (5.3c)$$

where

$$\mathcal{M}_I := I \otimes M,$$

$$\mathcal{F}^d := \mathbf{g}_0 \otimes \mathbf{y}^d \text{ with } \mathbf{y}^d(s) = \sum_{K \in \mathcal{T}_h} \int_K y^d \varphi_s \, d\mathbf{x},$$

$$\mathcal{M}_\gamma := (\mathcal{G}_0 \otimes M) + \gamma (\mathcal{M}_0 \otimes M) \text{ with } \mathcal{M}_0 = \text{diag} \left(0, \langle \psi_1 \rangle^2, \dots, \langle \psi_{J-1} \rangle^2 \right),$$

and $\mathbb{1}_{A^-}$, $\mathbb{1}_{A^+}$, and $\mathbb{1}_{\mathcal{I}}$ correspond to the characteristic functions of A^- , A^+ , and \mathcal{I} , respectively. Equivalently, \mathcal{M}_γ can be rewritten as

$$\mathcal{M}_\gamma := \mathcal{G}_\gamma \otimes M, \quad \text{with } \mathcal{G}_\gamma := \mathcal{G}_0 + \gamma \mathcal{M}_0,$$

where

$$\mathcal{G}_\gamma(r, s) = \begin{cases} \langle \psi_0 \rangle^2, & \text{if } r = s = 0, \\ (1 + \gamma) \langle \psi_r \rangle^2, & \text{if } r = s = 1, \dots, J-1, \\ 0, & \text{otherwise.} \end{cases} \quad (5.4)$$

Rearranging (5.3) gives us the following linear matrix system

$$\begin{bmatrix} \mathcal{M}_\gamma & 0 & -\mathcal{A}^* \\ 0 & \mu (\mathcal{G}_0 \otimes I) & \mathcal{G}_0 \otimes \text{diag}(\mathbb{1}_{\mathcal{I}}) \\ -\mathcal{A} & \mathcal{M}_I & 0 \end{bmatrix} \begin{bmatrix} \mathbf{y} \\ \mathbf{u} \\ \mathbf{p} \end{bmatrix} = \begin{bmatrix} \mathcal{F}^d \\ \mu ((\mathbf{g}_0 \otimes \mathbb{1}_{A^-}) \mathbf{u}_a + (\mathbf{g}_0 \otimes \mathbb{1}_{A^+}) \mathbf{u}_b) \\ -\mathcal{F} \end{bmatrix}, \quad (5.5)$$

which is a saddle point system. We note that since Legendre polynomials are used, $\mathcal{G}_0 = I$, and hence, $\mathcal{M}_I = \mathcal{M}$.

In practical implementations, the saddle point system (5.5) typically becomes very large, depending on the length of the random vector ξ and the number of refinement in the spatial discretization. We break this curse of dimensionality by using a low-rank approximation, which reduces both the

computational complexity and memory requirements by using a Kronecker-product structure of the matrices defined in (5.5).

5.3 Low-rank approach

We first introduce the notation and some basic properties of the low-rank approach. Let $\Theta = [\theta_1, \dots, \theta_J] \in \mathbb{R}^{N_d \times J}$ and let the operators $\text{vec}(\cdot)$ and $\text{mat}(\cdot)$ be isomorphic mappings between $\mathbb{R}^{N_d \times J}$ and $\mathbb{R}^{N_d J}$ as following

$$\text{vec} : \mathbb{R}^{N_d \times J} \rightarrow \mathbb{R}^{N_d J}, \quad \text{mat} : \mathbb{R}^{N_d J} \rightarrow \mathbb{R}^{N_d \times J},$$

where N_d and J are the degrees of freedom for the spatial discretization and the total degree of the multivariate stochastic basis polynomials, respectively. The matrix inner product is defined by $\langle U, V \rangle_F = \text{trace}(U^T V)$ with $\|U\|_F = \sqrt{\langle U, U \rangle_F}$. Further, the following relation holds, see, e.g., [36]:

$$\text{vec}(U\Theta V) = (V^T \otimes U)\text{vec}(\Theta). \quad (5.6)$$

Now, we can interpret the system (5.5) as follows

$$\underbrace{\begin{bmatrix} \mathcal{G}_\gamma \otimes M & 0 & -\sum_{i=0}^N \mathcal{G}_i \otimes \mathcal{K}_i^* \\ 0 & \mu(\mathcal{G}_0 \otimes I) & \mathcal{G}_0 \otimes \text{diag}(\mathbb{1}_I) \\ -\sum_{i=0}^N \mathcal{G}_i \otimes \mathcal{K}_i & \mathcal{G}_0 \otimes M & 0 \end{bmatrix}}_{\mathcal{L}} \underbrace{\begin{bmatrix} \text{vec}(Y) \\ \text{vec}(U) \\ \text{vec}(P) \end{bmatrix}}_{\Theta} = \underbrace{\begin{bmatrix} \text{vec}(B_1) \\ \text{vec}(B_2) \\ \text{vec}(B_3) \end{bmatrix}}_{\mathcal{B}}, \quad (5.7)$$

where

$$Y = (y_0, \dots, y_{J-1}), \quad U = (u_0, \dots, u_{J-1}), \quad P = (p_0, \dots, p_{J-1}), \quad B_1 = \text{mat}(\mathcal{F}^d), \\ B_2 = \text{mat}(\mu((\mathbf{g}_0 \otimes \mathbb{1}_{A^-}) \mathbf{u}_a + (\mathbf{g}_0 \otimes \mathbb{1}_{A^+}) \mathbf{u}_b)), \quad B_3 = \text{mat}(-\mathcal{F}).$$

By the identity (5.6), we have

$$\mathcal{L}\Theta = \text{vec} \left(\begin{bmatrix} MY\mathcal{G}_\gamma^T - \sum_{i=0}^N \mathcal{K}_i^* P\mathcal{G}_i^T \\ \mu IU\mathcal{G}_0^T + \text{diag}(\mathbb{1}_I)P\mathcal{G}_0^T \\ -\sum_{i=0}^N \mathcal{K}_i Y\mathcal{G}_i^T + MU\mathcal{G}_0^T \end{bmatrix} \right) = \text{vec} \left(\begin{bmatrix} B_1 \\ B_2 \\ B_3 \end{bmatrix} \right). \quad (5.8)$$

Assuming that the matrices Θ and \mathcal{B} have the following low-rank representations, see, e.g., [37, 61, 62],

$$Y = W_Y V_Y^T, \quad W_Y \in \mathbb{R}^{N_d \times r_Y}, \quad V_Y \in \mathbb{R}^{J \times r_Y}, \\ U = W_U V_U^T, \quad W_U \in \mathbb{R}^{N_d \times r_U}, \quad V_U \in \mathbb{R}^{J \times r_U}, \quad (5.9)$$

$$\begin{aligned}
P &= W_P V_P^T, & W_P &\in \mathbb{R}^{N_d \times r_P}, \quad V_P \in \mathbb{R}^{J \times r_P}, \\
B_1 &= B_{11} B_{12}^T & B_{11} &\in \mathbb{R}^{N_d \times r_{B_1}}, \quad B_{12} \in \mathbb{R}^{J \times r_{B_1}}, \\
B_2 &= B_{21} B_{22}^T & B_{21} &\in \mathbb{R}^{N_d \times r_{B_2}}, \quad B_{22} \in \mathbb{R}^{J \times r_{B_2}}, \\
B_3 &= B_{31} B_{32}^T & B_{31} &\in \mathbb{R}^{N_d \times r_{B_3}}, \quad B_{32} \in \mathbb{R}^{J \times r_{B_3}},
\end{aligned}$$

with $r_Y, r_U, r_P, r_{B_1}, r_{B_2}, r_{B_3} \ll N_d, J$, (5.8) can be stated as follows

$$\begin{bmatrix} MW_Y V_Y^T \mathcal{G}_\gamma^T - \sum_{i=0}^N \mathcal{K}_i^* W_P V_P^T \mathcal{G}_i^T \\ \mu I W_U V_U^T \mathcal{G}_0^T + \text{diag}(\mathbb{1}_I) W_P V_P^T \mathcal{G}_0^T \\ - \sum_{i=0}^N \mathcal{K}_i W_Y V_Y^T \mathcal{G}_i^T + M W_U V_U^T \mathcal{G}_0^T \end{bmatrix} = \begin{bmatrix} B_{11} B_{12}^T \\ B_{21} B_{22}^T \\ B_{31} B_{32}^T \end{bmatrix}, \quad (5.10)$$

where vec operator is ignored. Moreover, the three block rows in (5.10) can be written as

$$\underbrace{\left[MW_Y - \sum_{i=0}^N \mathcal{K}_i^* W_P \right]}_{\widehat{W}_1} \underbrace{[\mathcal{G}_\gamma V_Y \quad \mathcal{G}_i V_P]^T}_{\widehat{V}_1^T}, \quad (5.11a)$$

$$\underbrace{[\mu I W_U \quad \text{diag}(\mathbb{1}_I) W_P]}_{\widehat{W}_2} \underbrace{[\mathcal{G}_0 V_U \quad \mathcal{G}_0 V_P]^T}_{\widehat{V}_2^T}, \quad (5.11b)$$

$$\underbrace{\left[- \sum_{i=0}^N \mathcal{K}_i W_Y \quad M W_U \right]}_{\widehat{W}_3} \underbrace{[\mathcal{G}_i V_Y \quad \mathcal{G}_0 V_U]^T}_{\widehat{V}_3^T}, \quad (5.11c)$$

in low-rank formats $\widehat{W}_i \widehat{V}_i^T$ for $i = 1, 2, 3$. By the usage of (5.11), the low-rank approximate solutions to (5.7) can be obtained; see Algorithm 1 modified from [62] for details of the low-rank implementation of GMRES. Moreover, with the help of the following fact

$$\text{trace}(A^T B) = \text{vec}(A)^T \text{vec}(B),$$

the inner products $\langle A, B \rangle_F = \text{trace}(A^T B)$ in the iterative low-rank algorithm can be computed efficiently. For instance, the inner product computation in Algorithm 1 denoted by

$$\text{trprod}(A_{11}, A_{12}, A_{21}, A_{22}, A_{31}, A_{32}, B_{11}, B_{12}, B_{21}, B_{22}, B_{31}, B_{32})$$

can be computed as following

$$\langle A, B \rangle_F = \text{trace} \left((A_{11} A_{12}^T)^T (B_{11} B_{12}^T)^T \right) + \text{trace} \left((A_{21} A_{22}^T)^T (B_{21} B_{22}^T)^T \right)$$

$$\begin{aligned}
& + \text{trace} \left((A_{31} A_{32}^T)^T (B_{31} B_{32}^T)^T \right) \\
& = \text{trace} (A_{11}^T B_{11} A_{12}^T B_{12}) + \text{trace} (A_{21}^T B_{21} A_{22}^T B_{22}) \\
& + \text{trace} (A_{31}^T B_{31} A_{32}^T B_{32}),
\end{aligned}$$

where

$$A = \text{vec} \left(\begin{bmatrix} A_{11} A_{12}^T \\ A_{21} A_{22}^T \\ A_{31} A_{32}^T \end{bmatrix} \right), \quad B = \text{vec} \left(\begin{bmatrix} B_{11} B_{12}^T \\ B_{21} B_{22}^T \\ B_{31} B_{32}^T \end{bmatrix} \right).$$

During the iteration process, the rank of low-rank factors can increase either via matrix vector products or vector (matrix) additions. Thus, the cost of rank-reduction techniques is kept under control by using truncation based on singular values [36] or truncation based on coarse-grid rank reduction [63]. Our approach is based on the discussion in [37, 64], where a truncated SVD of $U = W^T V \approx B \text{diag}(\sigma_1, \dots, \sigma_r) C^T$ is constructed for the largest r singular values, which are greater than the given truncation tolerance ϵ_{trunc} . In Algorithm 1, this process is done by the truncation operator \mathcal{T} . Further, in the numerical simulations, a rather small truncation tolerance ϵ_{trunc} is used to represent the full-rank solution as accurate as possible.

We know that iterative methods such as GMRES exhibit a better convergence in terms of the number of iterations when they are used with a suitable preconditioner. The low-rank variants also display the same behaviour so that we use a block diagonal mean-based preconditioner of the form

$$\mathcal{P}_0 = \begin{bmatrix} \mathcal{M}_\gamma & 0 & 0 \\ 0 & \mu (\mathcal{G}_0 \otimes I) & 0 \\ 0 & 0 & \tilde{S} \end{bmatrix},$$

where $\tilde{S} = (\mathcal{G}_0 \otimes \tilde{\mathcal{K}}_0) \mathcal{M}_\gamma^{-1} (\mathcal{G}_0 \otimes \tilde{\mathcal{K}}_0)^T$ corresponds to the approximated Schur complement with $\tilde{\mathcal{K}}_0 = \mathcal{K}_0 + \sqrt{\frac{1+\gamma}{\mu}} M \text{diag}(\mathbb{1}_{\mathcal{I}})$; see, e.g., [14, 49].

6 Numerical Results

This section contains a set of numerical experiments to illustrate the performance of proposed discretization techniques and a low-rank variant of GMRES approach. All numerical simulations are done in MATLAB R2021a on an Ubuntu Linux machine with 32 GB RAM. Iterative approaches are ended when the residual becomes smaller than the given tolerance value $\epsilon_{tol} = 5 \times 10^{-3}$ or the maximum iteration number ($\#iter_{max} = 250$) is reached. The truncation tolerance $\epsilon_{trunc} = 10^{-8}$ is chosen, such that $\epsilon_{trunc} \leq \epsilon_{tol}$; otherwise, one would iterate the noise during the low-rank process.

Algorithm 1 Low-rank preconditioned GMRES (LRPGMRES)

Input: Coefficient matrix $\mathcal{L} : \mathbb{R}^{3Nd \times J} \rightarrow \mathbb{R}^{3Nd \times J}$, inverse of the preconditioner matrix $\mathcal{P}_0^{-1} : \mathbb{R}^{3Nd \times J} \rightarrow \mathbb{R}^{3Nd \times J}$, and right-hand side matrix \mathcal{B} in the low-rank formats. Truncation operator \mathcal{T} with given tolerance ϵ_{trunc} .

Output: Matrix $\Theta \in \mathbb{R}^{3Nd \times J}$ satisfying $\|\mathcal{L}(\Theta) - \mathcal{B}\|_F / \|\mathcal{B}\|_F \leq \epsilon_{tol}$.

```

1: Choose initial guess  $\Theta_{11}^{(0)}, \Theta_{12}^{(0)}, \Theta_{21}^{(0)}, \Theta_{22}^{(0)}, \Theta_{31}^{(0)}, \Theta_{33}^{(0)}$ .
2:  $(\tilde{\Theta}_{11}, \tilde{\Theta}_{12}, \tilde{\Theta}_{21}, \tilde{\Theta}_{22}, \tilde{\Theta}_{31}, \tilde{\Theta}_{32}) = \mathcal{L}(\Theta_{11}^{(0)}, \Theta_{12}^{(0)}, \Theta_{21}^{(0)}, \Theta_{22}^{(0)}, \Theta_{31}^{(0)}, \Theta_{32}^{(0)})$ .  $\tilde{\Theta}_{ij} \leftarrow \mathcal{T}(\tilde{\Theta}_{ij})$ 
3:  $R_{11}^{(0)} = \{B_{11}, -\Theta_{11}^{(0)}\}$ ,  $R_{12}^{(0)} = \{B_{12}, \Theta_{12}^{(0)}\}$ .
4:  $R_{21}^{(0)} = \{B_{21}, -\Theta_{21}^{(0)}\}$ ,  $R_{22}^{(0)} = \{B_{22}, \Theta_{22}^{(0)}\}$ .  $R_{ij}^{(0)} \leftarrow \mathcal{T}(R_{ij}^{(0)})$ 
5:  $R_{31}^{(0)} = \{B_{31}, -\Theta_{31}^{(0)}\}$ ,  $R_{32}^{(0)} = \{B_{32}, \Theta_{32}^{(0)}\}$ .
6:  $\|R^0\| = \sqrt{\text{trprod}(R_{11}^{(0)}, \dots, R_{11}^{(0)}, \dots)}$ .
7:  $V_{11}^{(0)} = R_{11}^{(0)} / \|R^0\|_F$ ,  $V_{12}^{(0)} = R_{12}^{(0)}$ .
8:  $V_{21}^{(0)} = R_{21}^{(0)} / \|R^0\|_F$ ,  $V_{22}^{(0)} = R_{22}^{(0)}$ .  $V_{ij}^{(0)} \leftarrow \mathcal{T}(V_{ij}^{(0)})$ 
9:  $V_{31}^{(0)} = R_{31}^{(0)} / \|R^0\|_F$ ,  $V_{32}^{(0)} = R_{32}^{(0)}$ .
10:  $\gamma = [\gamma_1, 0, \dots, 0]$ ,  $\gamma_1 = \sqrt{\text{trprod}(V_{11}^{(0)}, \dots, V_{11}^{(0)}, \dots)}$ .
11: while  $i \leq \text{maxit}$  do
12:  $(Z_{11}^{(i)}, Z_{12}^{(i)}, Z_{21}^{(i)}, Z_{22}^{(i)}, Z_{31}^{(i)}, Z_{32}^{(i)}) = \mathcal{P}_0^{-1}(V_{11}^{(i)}, V_{12}^{(i)}, V_{21}^{(i)}, V_{22}^{(i)}, V_{31}^{(i)}, V_{32}^{(i)})$ ,  $Z_{ij}^{(i)} \leftarrow \mathcal{T}(Z_{ij}^{(i)})$ 
13:  $(W_{11}, W_{12}, W_{21}, W_{22}, W_{31}, W_{32}) = \mathcal{L}(Z_{11}^{(i)}, Z_{12}^{(i)}, Z_{21}^{(i)}, Z_{22}^{(i)}, Z_{31}^{(i)}, Z_{32}^{(i)})$ .  $W_{ij} \leftarrow \mathcal{T}(W_{ij})$ 
14: for  $j = 1, \dots, i$  do
15:  $m_{j,i} = \sqrt{\text{trprod}(W_{11}, \dots, V_{11}^{(j)}, \dots)}$ 
16:  $W_{11} = \{W_{11}, -m_{j,i}V_{11}^{(i)}\}$ ,  $W_{12} = \{W_{12}, V_{12}^{(j)}\}$ .
17:  $W_{21} = \{W_{21}, -m_{j,i}V_{21}^{(i)}\}$ ,  $W_{22} = \{W_{22}, V_{22}^{(j)}\}$ .  $W_{ij} \leftarrow \mathcal{T}(W_{ij})$ 
18:  $W_{31} = \{W_{31}, -m_{j,i}V_{31}^{(i)}\}$ ,  $W_{32} = \{W_{32}, V_{32}^{(j)}\}$ .
19: end for
20:  $m_{i+1,i} = \sqrt{\text{trprod}(W_{11}, \dots, W_{11}, \dots)}$ 
21:  $V_{11}^{(i+1)} = W_{11} / m_{i+1,i}$ ,  $V_{12}^{(k+1)} = W_{12}$ .
22:  $V_{21}^{(i+1)} = W_{21} / m_{i+1,i}$ ,  $V_{22}^{(k+1)} = W_{22}$ .  $V_{ij}^{(i+1)} \leftarrow \mathcal{T}(V_{ij}^{(i+1)})$ 
23:  $V_{31}^{(i+1)} = W_{31} / m_{i+1,i}$ ,  $V_{32}^{(k+1)} = W_{32}$ .
24: Perform Givens rotations for the  $i$ th column of  $m$ :
25: for  $j = 1, \dots, i-1$  do
26:  $\begin{bmatrix} m_{j,i} \\ m_{j+1,i} \end{bmatrix} = \begin{bmatrix} c_j & s_j \\ -s_j & c_j \end{bmatrix} \begin{bmatrix} m_{j,i} \\ m_{j+1,i} \end{bmatrix}$ 
27: end for
28: Compute  $i$ th Givens rotation, and perform for  $\gamma$  and last column of  $m$ .
29:  $\begin{bmatrix} \gamma_i \\ \gamma_{i+1} \end{bmatrix} = \begin{bmatrix} c_i & s_i \\ -s_i & c_i \end{bmatrix} \begin{bmatrix} \gamma_i \\ 0 \end{bmatrix}$ 
30:  $m_{i,i} = c_i m_{i,i} + s_i m_{i+1,i}$ ,  $m_{i+1,i} = 0$ .
31: if  $|\gamma_{i+1}| \leq \epsilon_{tol}$  then
32: Compute  $y$  from  $My = \xi$ , where  $(M)_{j,i} = m_{j,i}$ .
33:  $Y_{11} = \{y_1 V_{11}^{(1)}, \dots, y_k V_{11}^{(i)}\}$ ,  $Y_{12} = \{V_{12}^{(1)}, \dots, V_{12}^{(i)}\}$ .
34:  $Y_{21} = \{y_1 V_{21}^{(1)}, \dots, y_k V_{21}^{(i)}\}$ ,  $Y_{22} = \{V_{22}^{(1)}, \dots, V_{22}^{(i)}\}$ .  $Y_{ij} \leftarrow \mathcal{T}(Y_{ij})$ 
35:  $Y_{31} = \{y_1 V_{31}^{(1)}, \dots, y_k V_{31}^{(i)}\}$ ,  $Y_{32} = \{V_{32}^{(1)}, \dots, V_{32}^{(i)}\}$ .
36:  $(\tilde{Y}_{11}, \tilde{Y}_{12}, \tilde{Y}_{21}, \tilde{Y}_{22}, \tilde{Y}_{31}, \tilde{Y}_{32}) = \mathcal{P}_0^{-1}(Y_{11}, Y_{12}, Y_{21}, Y_{22}, Y_{31}, Y_{32})$ .  $\tilde{Y}_{ij} \leftarrow \mathcal{T}(\tilde{Y}_{ij})$ 
37:  $\Theta_{11} = \{\Theta_{11}^{(0)}, \tilde{Y}_{11}\}$ ,  $\Theta_{12} = \{\Theta_{12}^{(0)}, \tilde{Y}_{12}\}$ .
38:  $\Theta_{21} = \{\Theta_{21}^{(0)}, \tilde{Y}_{21}\}$ ,  $\Theta_{22} = \{\Theta_{22}^{(0)}, \tilde{Y}_{22}\}$ .  $\Theta_{ij} \leftarrow \mathcal{T}(\Theta_{ij})$ 
39:  $\Theta_{31} = \{\Theta_{31}^{(0)}, \tilde{Y}_{31}\}$ ,  $\Theta_{32} = \{\Theta_{32}^{(0)}, \tilde{Y}_{32}\}$ .
40: end if
41: end while

```

In the numerical experiments, the random coefficient η is described by the following covariance function

$$\mathbb{C}_\eta(\mathbf{x}, \mathbf{y}) = \kappa^2 \prod_{n=1}^2 e^{-|x_n - y_n| / \ell_n}, \quad \forall(\mathbf{x}, \mathbf{y}) \in \mathcal{D} \quad (6.1)$$

with the correlation length ℓ_n . Linear elements are used to generate discontinuous Galerkin basis, whereas Legendre polynomials are taken as the stochastic basis functions since the underlying random variables have uniform distribution over $[-\sqrt{3}, \sqrt{3}]$, that is, $\xi_j \sim \mathcal{U}[-\sqrt{3}, \sqrt{3}]$, $j = 1, \dots, N$. Explicit eigenpairs (λ_j, ϕ_j) of the covariance function (6.1) can be found in [44]. Further, all parameters used in the simulations are described in Table 1.

Table 1: Descriptions of the parameters used in the simulations.

Parameter	Description
N_d	degrees of freedom for the spatial discretization
N	truncation number in KL expansion
Q	highest order of basis polynomials for the stochastic domain
μ	regularization parameter of the control u
γ	risk-aversion parameter
ν	viscosity parameter
ℓ	correlation length
κ	standard deviation

6.1 Unconstrained problem with random diffusion parameter

As a first benchmark problem, we consider an unconstrained optimal control problem, that is, $\mathcal{U}^{ad} = \mathcal{U}$, having a random diffusion coefficient defined on $\mathcal{D} = [-1, 1]^2$ with the source function $f(\mathbf{x}) = 0$, the convection parameter $\mathbf{b}(\mathbf{x}) = (0, 1)^T$, and the Dirichlet boundary condition

$$y_{DB}(\mathbf{x}) = \begin{cases} y_{DB}(x_1, -1) = x_1, & y_{DB}(x_1, 1) = 0, \\ y_{DB}(-1, x_2) = -1, & y_{DB}(1, x_2) = 1. \end{cases}$$

The random diffusion parameter is chosen as $a(\mathbf{x}, \omega) = \nu \eta(\mathbf{x}, \omega)$, where the random field $\eta(\mathbf{x}, \omega)$ has the unity mean with the corresponding covariance function (6.1) and ν is the viscosity parameter. The desired state (or target) y^d corresponds to the stochastic solution of the forward model by taking $u(\mathbf{x}) = 0$. The desired state exhibits exponential boundary layer near $x_2 = 1$, where the solution changes in a dramatic manner. Therefore, the boundary layer becomes more visible as ν decreases; see Figure 1 for the mean of the state $\mathbb{E}[y_h]$, the desired state y^d , and the corresponding control u_h for various values of the viscosity parameter ν .

Table 2 shows the values of the cost functional $\mathcal{J}(u_h)$ and tracking term $\|y_h - y^d\|_{\mathcal{X}}^2$ obtained by $\mathcal{L} \backslash \mathcal{B}$ for various values of the viscosity parameter ν and the regularization parameter μ . We observe that the tracking term and the objective functional become smaller as μ decreases. Moreover, Table 3 exhibits that the peak values of states' variance can be reduced by increasing the value of the parameter γ .

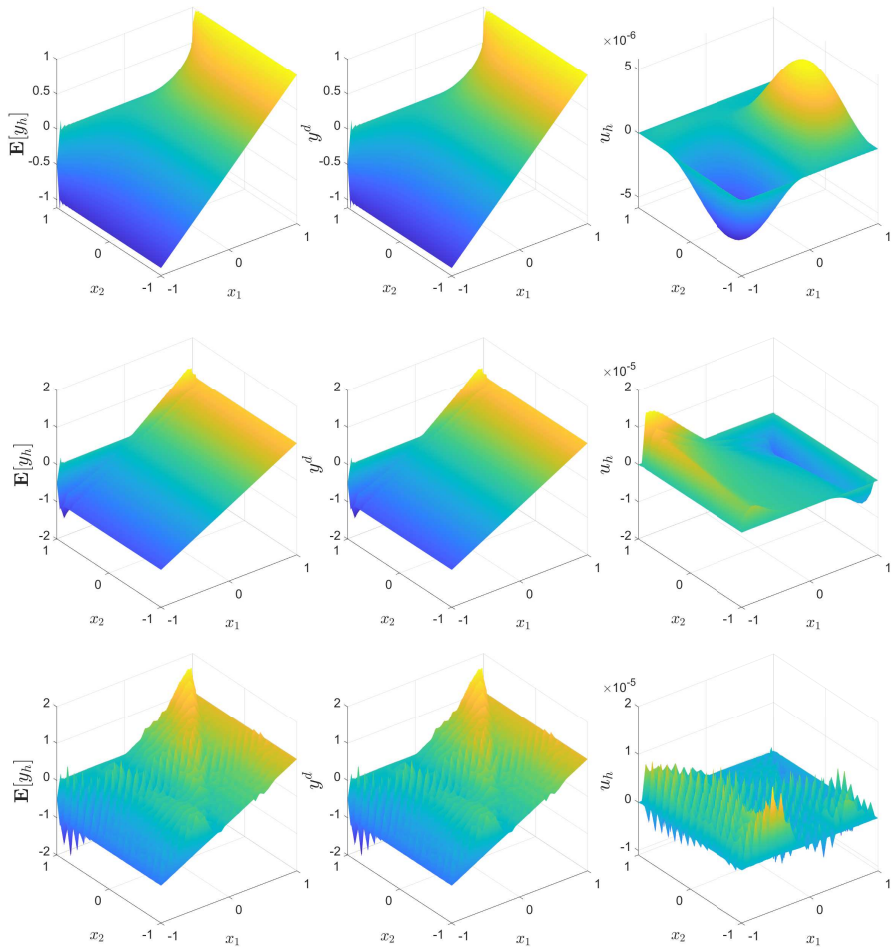


Fig. 1: Example 6.1: Simulations of the mean of state $\mathbb{E}[y_h]$, the desired state (target) y^d , and the control u_h (from left to right) obtained by $\mathcal{L}\backslash\mathcal{B}$ with $N_d = 6144$, $N = 3$, $Q = 3$, $\ell = 1$, $\kappa = 0.05$, $\mu = 1$, and $\gamma = 1$ for varying $\nu = 1, 10^{-2}, 10^{-4}$ (from top to bottom).

Next, we display the performance of $\mathcal{L}\backslash\mathcal{B}$ in terms of total CPU times (in seconds) and storage requirements (in KB) in Table 4. However, we could not report some numerical results since the simulation is ended with “out of memory”, which we have denoted as “OoM”. To handle the curse of dimensionality and so increase the value of truncation number N , we need effective numerical approaches or solvers such as a low-rank variant of GMRES iteration with a mean based preconditioner discussed in Section 5.3.

Table 5 reports the results of the simulations by considering various data sets in the low-rank format. By keeping other parameters fixed, we show results

Table 2: Example 6.1: Computational values of the cost functional $\mathcal{J}(u_h)$ and tracking term $\|y_h - y^d\|_{\mathcal{X}}^2$ obtained by $\mathcal{L} \setminus \mathcal{B}$ with $N_d = 6144$, $N = 3$, $Q = 3$, $\ell = 1$, $\kappa = 0.5$, and $\gamma = 1$ for varying values of the viscosity parameter ν and the regularization parameter μ .

		$\mu = 1$	$\mu = 10^{-2}$	$\mu = 10^{-4}$	$\mu = 10^{-6}$
$\nu = 1$	$\mathcal{J}(u_h)$	1.2393e-05	2.5034e-06	1.0257e-06	9.7533e-07
	$\ y_h - y^d\ _{\mathcal{X}}^2$	5.4679e-06	7.1725e-07	3.2113e-08	1.6931e-09
$\nu = 10^{-2}$	$\mathcal{J}(u_h)$	1.4349e-05	8.3285e-06	7.2067e-07	6.0683e-07
	$\ y_h - y^d\ _{\mathcal{X}}^2$	1.3120e-05	4.1452e-06	9.0731e-08	3.5983e-09
$\nu = 10^{-4}$	$\mathcal{J}(u_h)$	1.3675e-05	1.1798e-06	3.9380e-07	3.7211e-07
	$\ y_h - y^d\ _{\mathcal{X}}^2$	1.5285e-05	4.3924e-07	1.1422e-07	8.3896e-09

Table 3: Example 6.1: Peak values of the states' variance obtained by $\mathcal{L} \setminus \mathcal{B}$ with $N_d = 6144$, $N = 3$, $Q = 3$, $\ell = 1$, $\nu = 1$, and $\mu = 1$ for varying values of the risk-aversion γ and the standard deviation κ .

	$\kappa = 0.05$	$\kappa = 0.25$	$\kappa = 0.5$
$\gamma = 0$	4.5406e-05	1.1980e-03	5.7995e-03
$\gamma = 1$	4.1995e-05	1.0984e-03	5.1327e-03
$\gamma = 2$	3.8944e-05	1.0110e-03	4.5807e-03
$\gamma = 3$	3.6207e-05	9.3377e-04	4.1243e-03
$\gamma = 4$	3.3731e-05	8.6520e-04	3.7409e-03

Table 4: Example 6.1: Total CPU times (in seconds) and memory (in KB) for $N_d = 6144$, $Q = 3$, $\ell = 1$, $\mu = 10^{-2}$, $\gamma = 1$, and $\kappa = 0.5$.

$\mathcal{L} \setminus \mathcal{B}$	$\nu = 10^0$	$\nu = 10^{-2}$	$\nu = 10^{-4}$
N	CPU (Memory)	CPU (Memory)	CPU (Memory)
2	116.0 (2880)	116.1 (2880)	117.5 (960)
3	779.6 (5760)	787.7 (5760)	813.0 (5760)
4	OoM	OoM	OoM

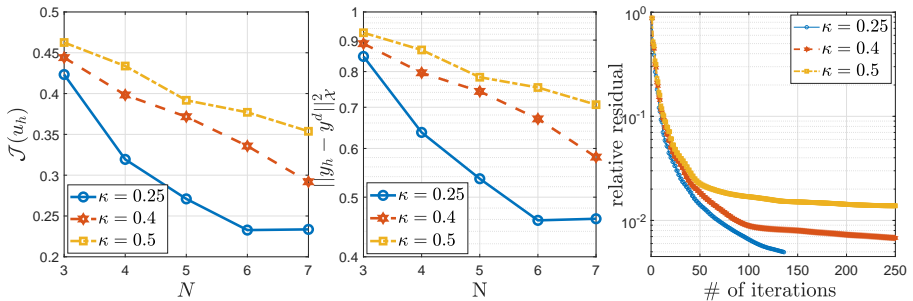


Fig. 2: Example 6.1: Behaviours of the cost functional $\mathcal{J}(u_h)$ (left), the tracking term $\|y_h - y^d\|_{\mathcal{X}}^2$ (middle), and the relative residual (right) with $N_d = 6144$, $Q = 3$, $\ell = 1$, $\nu = 1$, $\mu = 10^{-2}$, $\gamma = 0$, and the mean-based preconditioner \mathcal{P}_0 for varying values of κ .

Table 5: Example 6.1: Total number of iterations, total rank of the truncated solutions, total CPU times (in seconds), relative residual, and memory demand of the solution (in KB) with $N_d = 6144$, $Q = 3$, $\ell = 1$, $\kappa = 0.5$, $\nu = 1$, $\gamma = 0$, and the mean-based preconditioner \mathcal{P}_0 for varying values of N and μ .

		$\mu = 1$	$\mu = 10^{-2}$	$\mu = 10^{-4}$
$N = 4$	#iter	250	250	250
	Rank	51	51	51
	CPU	40126.1	40017.9	39950.4
	Resi.	3.5759e-02	3.3521e-02	3.7375e-02
	Memory	2461.9	2461.9	2461.9
$N = 5$	#iter	250	250	250
	Rank	84	84	84
	CPU	91366.2	90544.0	90021.2
	Resi.	2.1672e-02	2.3056e-02	3.1080e-02
	Memory	4068.8	4068.8	4068.8
$N = 6$	#iter	250	250	250
	Rank	126	126	126
	CPU	208643.4	207964.0	207464.4
	Resi.	1.8357e-02	1.8064e-02	2.0494e-02
	Memory	6130.7	6130.7	6130.7
$N = 7$	#iter	250	250	250
	Rank	180	180	180
	CPU	355115.9	355167.5	355652.3
	Resi.	1.1208e-02	1.3833e-02	1.4914e-02
	Memory	8808.8	8808.8	8808.8

for varying truncation number N in KL expansion and regularization parameter μ for $\kappa = 0.5$ in Table 5. When N increases, the complexity of the problem increases in terms of the number of rank, memory, and CPU time. Another key observation is that the relative residual decreases independently of the value of μ while increasing N .

Next, we investigate the effect of the standard deviation parameter κ on the numerical simulations. Figure 2 displays the behaviours of the cost functional $\mathcal{J}(u_h)$, the tracking term $\|y_h - y^d\|_{\mathcal{X}}^2$, and the relative residual for various values of κ . We observe that the values of $\mathcal{J}(u_h)$ and $\|y_h - y^d\|_{\mathcal{X}}^2$ decrease monotonically as the value of κ increases. Moreover, the low-rank variant of preconditioned GMRES method yields convergence behaviour for all values of κ . Lastly, Figure 3 shows that the speed of convergence of relative residual decreases by increasing the value of risk-aversion parameter γ in the beginning of the iteration.

6.2 Unconstrained problem with random convection parameter

Our second example is an unconstrained optimal control problem containing random velocity input parameter. To be precise, we set the deterministic diffusion parameter $a(\mathbf{x}, \omega) = \nu > 0$, the deterministic source function $f(\mathbf{x}) = 0$, and homogeneous Dirichlet boundary conditions on the spatial domain $\mathcal{D} =$

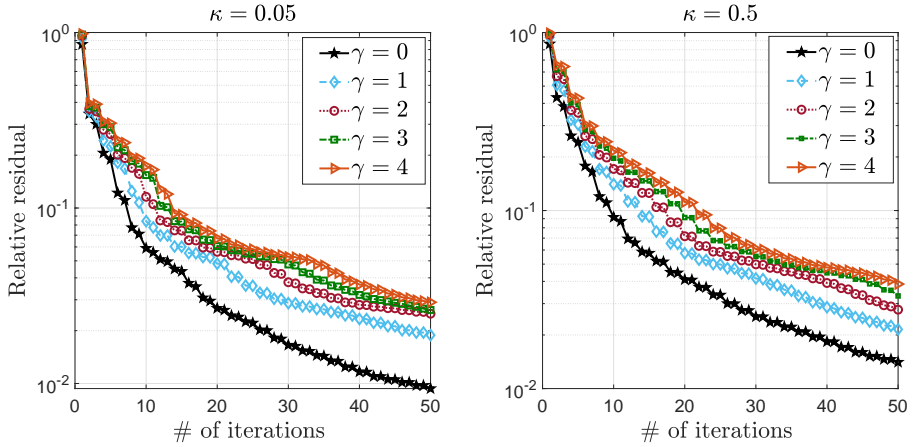


Fig. 3: Example 6.1: Convergence of LRPGMRES with $N_d = 6144$, $N = 5$, $Q = 3$, $\ell = 1$, $\mu = 1$, $\nu = 1$ for varying κ and γ .

$[-1, 1]^2$. On the other hand, the random velocity field $\mathbf{b}(\mathbf{x}, \omega)$ is defined as $\mathbf{b}(\mathbf{x}, \omega) = (\eta(\mathbf{x}, \omega), \eta(\mathbf{x}, \omega))^T$, where the random input $\eta(\mathbf{x}, \omega)$ has the unity mean, i.e., $\bar{\eta}(\mathbf{x}) = 1$. Further, the desired state y^d is given by

$$y^d(\mathbf{x}) = \exp \left[-64 \left(\left(x_1 - \frac{1}{2} \right)^2 + \left(x_2 - \frac{1}{2} \right)^2 \right) \right].$$

Figure 4 and 5 display, respectively, the mean of state $\mathbb{E}[y_h]$ and the control u_h for varied values of the regularization parameter μ obtained by solving the full-rank system $\mathcal{L}\mathcal{B}$. As the previous example, we observe that the state y_h becomes closer to the target solution y^d while μ decreases.

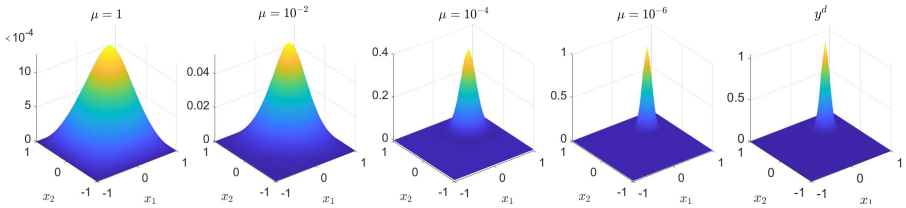


Fig. 4: Example 6.2: Simulations of the mean of state $\mathbb{E}[y_h]$ obtained by $\mathcal{L}\mathcal{B}$ with $N_d = 6144$, $N = 3$, $Q = 3$, $\ell = 1$, $\kappa = 0.05$, $\nu = 1$, and $\gamma = 0$ for varying $\mu = 1, 10^{-2}, 10^{-4}, 10^{-6}$ and the desired state y^d .

Next, we compare the full-rank solutions obtained by solving the system $\mathcal{L}\mathcal{B}$ with the low-rank ones. Figure 6 exhibits behaviours of the cost functionals $\mathcal{J}(u_h)$ (left), the tracking term $\|y_h - y^d\|_{\mathcal{X}}^2$ (middle), and the relative residual (right) for varying values of the regularization parameter μ . The key

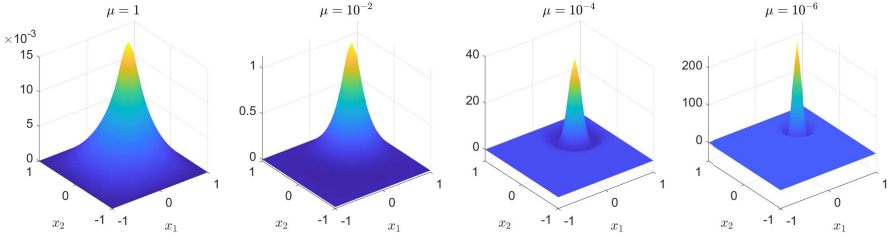


Fig. 5: Example 6.2: Simulations of the control u_h obtained solving by $\mathcal{L}\backslash\mathcal{B}$ with $N_d = 6144$, $N = 3$, $Q = 3$, $\ell = 1$, $\kappa = 0.05$, $\nu = 1$, and $\gamma = 0$ for varying regularization parameter $\mu = 1, 10^{-2}, 10^{-4}, 10^{-6}$.

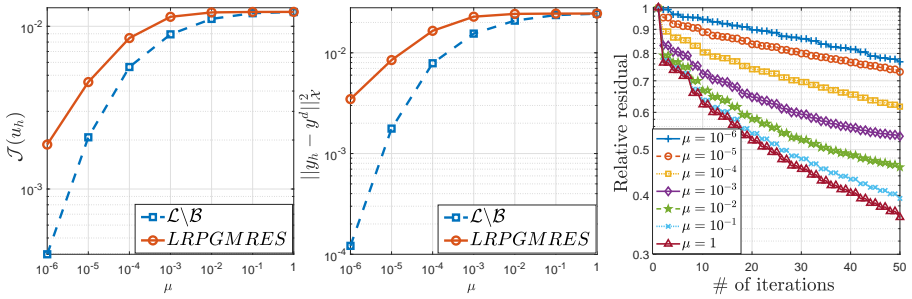


Fig. 6: Example 6.2: Behaviours of the cost functional $\mathcal{J}(u_h)$ (left), the tracking term $\|y_h - y^d\|_{\mathcal{X}}^2$ (middle), and the relative residual (right) with $N_d = 6144$, $N = 3$, $Q = 3$, $\kappa = 0.05$, $\ell = 1$, $\nu = 1$, $\gamma = 0$, and the mean-based preconditioner \mathcal{P}_0 for varying μ .

Table 6: Example 6.2: Simulation results showing total number of iterations, ranks of the truncated solutions, total CPU times (in seconds), relative residual, and memory demand of the solution (in KB) with $N_d = 6144$, $N = 3$, $Q = 3$, $\ell = 1$, $\nu = 1$, $\mu = 10^{-6}$, and the mean-based preconditioner \mathcal{P}_0 for varying γ .

	$\gamma = 0$	$\gamma = 10^{-6}$	$\gamma = 10^{-4}$	$\gamma = 10^{-2}$	$\gamma = 1$
#iter	250	250	250	250	250
Rank	29	30	30	30	21
CPU	24468.2	19383.2	17382.0	17422.8	17797.1
Resi.	2.1733e-01	2.6663e-01	4.0428e-01	6.9542e-01	9.1911e-01
Memory	1396.5	1444.7	1444.7	1444.7	963.2

observation is that the low-rank solutions display the same pattern with the full-rank solutions as μ increases. Moreover, Table 6 reports the results of the simulations by considering various values of the risk-aversion parameter γ . As the previous example, the relative residual becomes smaller as decreasing the value of γ .

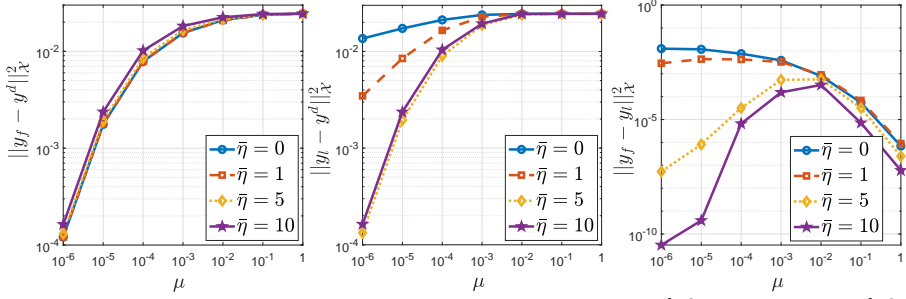


Fig. 7: Example 6.2: Behaviour of the differences $\|y_f - y^d\|_{\mathcal{X}}^2$ (left), $\|y_l - y^d\|_{\mathcal{X}}^2$ (middle), and $\|y_f - y_l\|_{\mathcal{X}}^2$ (right), where the full-rank and low-rank solutions are denoted by y_f and y_l , respectively, computed by solving the full-rank and low-rank systems with $N_d = 6144$, $N = 3$, $Q = 3$, $\ell = 1$, $\mu = 10^{-6}$, $\gamma = 0$, $\nu = 1$, and $\kappa = 0.05$ for varying values of the mean of random input $\eta(x)$.

Last, we investigate the effect of the mean of random input $\eta(x)$ on both full-rank and low-rank solutions. Denoting the full-rank solution and the low-rank solution by y_f and y_l , respectively, the behavior of the differences $\|y_f - y^d\|_{\mathcal{X}}^2$, $\|y_l - y^d\|_{\mathcal{X}}^2$, and $\|y_f - y_l\|_{\mathcal{X}}^2$ computed by solving the full-rank and low-rank systems is displayed in Figure 7. As increasing the mean of random input $\eta(x)$, the difference between the full-rank and low-rank solutions becomes smaller.

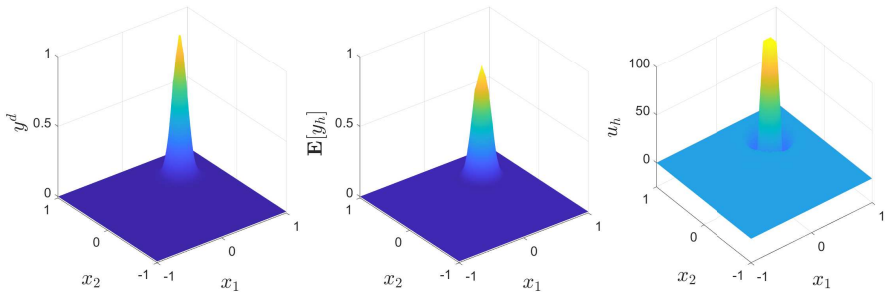


Fig. 8: Example 6.3: Simulations of the desired state y^d , the mean of state $\mathbb{E}[y_h]$, and the control u_h (from left to right) obtained by $\mathcal{L}\backslash\mathcal{B}$ with $N_d = 6144$, $N = 3$, $Q = 3$, $\ell = 1$, $\kappa = 0.05$, and $\nu = 1$.

6.3 Constrained problem with random convection parameter

Last, we consider a constrained optimal control problem containing a random velocity parameter. Except from the set up of Example 6.2, we have an upper bound for the control variable such as $u_b = 100$. Taking the results in the

Table 7: Example 6.3: Simulation results showing the memory demand of the solution (in KB), the objective function $\mathcal{J}(u_h)$, the tracking term $\|y_h - y^d\|_{\mathcal{X}}^2$, the difference of the full-rank and low-rank $\|y_f - y_l\|_{\mathcal{X}}^2$, ranks of the truncated solutions, and the relative residual with $N_d = 6144$, $Q = 3$, $\ell = 1$, $\nu = 1$, and the mean-based preconditioner \mathcal{P}_0 .

	Memory	$\mathcal{J}(u_h)$	$\ y_h - y^d\ _{\mathcal{X}}^2$	$\ y_f - y_l\ _{\mathcal{X}}^2$	Rank	Res.
$N = 3$	5744.0	5.508e-04	6.031e-04			
$N = 3$	1444.7	1.046e-02	2.091e-02	1.802e-02	30	9.232e-01
$N = 4$	2461.9	1.029e-02	2.056e-02	1.769e-02	51	9.161e-01
$N = 5$	4068.8	9.996e-03	1.996e-02	1.713e-02	84	9.042e-01
$N = 6$	6130.7	9.616e-03	1.919e-02	1.642e-02	126	8.895e-01

previous example into account, the regularization and risk-averse parameters are chosen as $\mu = 10^{-6}$ and $\gamma = 0$, respectively.

Figure 8 displays the desired state y^d , the mean of state $\mathbb{E}[y_h]$, and the control u_h obtained by $\mathcal{L} \backslash \mathcal{B}$. We observe that the upper bound of the control constrained is satisfied. In Table 7, we compare the low-rank solutions with the full-rank ones. As increasing the truncation number N , we obtain better results as expected.

7 Conclusions

In this paper, we have numerically studied the statistical moments of a robust deterministic optimal control problem subject to a convection diffusion equation having random coefficients. With the help of the stochastic discontinuous Galerkin method, we transform the original problem into a large system consisting of deterministic optimal control problems for each realization of the random coefficients. However, we could not obtain some numerical results when increasing the value of truncation number N . Therefore, to reduce computational time and memory requirements, we have used a low-rank variant of GMRES iteration with a mean based preconditioner (LRPGMRES). It has been shown in the numerical simulations that LRPGMRES can be an alternative to solve such large systems. As a future study, randomness can be considered in different forms, for instance, in boundary conditions, desired state, or geometry. Moreover, to handle curse of dimensionality, reduced order models, see, e.g., [65, 66], can be an alternative to the low-rank approximations.

Funding. This work was supported by TUBITAK 1001 Scientific and Technological Research Projects Funding Program with project number 119F022. The authors would also like to express their sincere thanks to the anonymous referees for their most valuable suggestions.

Declarations

Conflict of interest. The authors declare no competing interests.

References

- [1] Roache, P.J.: *Verification & Validation in Computational Science and Engineering*. Hermosa Publishers, Albuquerque, NM (1998)
- [2] Borzi, A.: Multigrid and sparse-grid schemes for elliptic control problems with random coefficients. *Comput. Vis. Sci.* **13**, 153–160 (2010)
- [3] Borzi, A., Schulz, V., Schillings, C., von Winckel, G.: On the treatment of distributed uncertainties in PDE constrained optimization. *GAMM Mitteilungen* **33**(2), 230–246 (2010)
- [4] Negri, F., Manzoni, A., Rozza, G.: Reduced basis approximation of parametrized optimal flow control problems for the Stokes equations. *Comput. Math. Appl.* **69**(4), 319–336 (2015)
- [5] Ali, A.A., Ullmann, E., Hinze, M.: Multilevel Monte Carlo analysis for optimal control of elliptic PDEs with random coefficients. *SIAM/ASA J. Uncertain. Quantif.* **5**, 466–492 (2017)
- [6] Lazar, M., Zuazua, E.: Averaged control and observation of parameter-depending wave equations. *C. R. Math. Acad. Sci. Paris* **352**, 497–502 (2014)
- [7] Zuazua, E.: Averaged control. *Automatica* **50**(12), 3077–3087 (2014)
- [8] Garreis, S., Ulbrich, M.: Constrained optimization with low-rank tensors and applications to parametric problems with PDEs. *SIAM J. Sci. Comput.* **39**, 25–54 (2017)
- [9] Gunzburger, M.D., Lee, H.-C., Lee, J.: Error estimates of stochastic optimal Neumann boundary control problems. *SIAM J. Numer. Anal.* **49**(4), 1532–1552 (2011)
- [10] Hou, L.S., Lee, J., Manouzi, H.: Finite element approximations of stochastic optimal control problems constrained by stochastic elliptic PDEs. *J. Math. Anal. Appl.* **384**, 87–103 (2011)
- [11] Kouri, D.P., Heinkenschloss, M., Ridzal, D., van Bloemen Waanders, B.G.: A trust-region algorithm with adaptive stochastic collocation for PDE optimization under uncertainty. *SIAM J. Sci. Comput.* **35**, 1847–1879 (2013)
- [12] Lee, H.-C., Lee, J.: A stochastic Galerkin method for stochastic control problems. *Commun. Comput. Phys.* **14**, 77–106 (2013)
- [13] Rosseel, E., Wells, G.N.: Optimal control with stochastic PDE constraints and uncertain controls. *Comput. Methods Appl. Mech. Engrg.* **213/216**,

152–167 (2012)

- [14] Benner, P., Onwunta, A., Stoll, M.: Block-diagonal preconditioning for optimal control problems constrained by PDEs with uncertain inputs. *SIAM. J. Matrix Anal. & Appl.* **37**, 491–518 (2016)
- [15] Chen, P., Quarteroni, A., Rozza, G.: Stochastic optimal Robin boundary control problems of advection-dominated elliptic equations. *SIAM J. Numer. Anal.* **51**, 2700–2722 (2013)
- [16] Kunoth, A., Schwab, C.: Sparse adaptive tensor Galerkin approximations of stochastic PDE-constrained control problems. *SIAM/ASA J. Uncertain. Quantif.* **4**, 1034–1059 (2016)
- [17] Tiesler, H., Kirby, R.M., Xiu, D., Preusser, T.: Stochastic collocation for optimal control problems with stochastic PDE constraints. *SIAM J. Control Optim.* **50**(5), 2659–2682 (2012)
- [18] Guth, P.A., Kaarnioja, V., Kuo, F.Y., Schillings, C., Sloan, I.H.: A quasi-Monte Carlo method for optimal control under uncertainty. *SIAM/ASA J. Uncertain. Quantif.* **9**(2), 354–383 (2021)
- [19] Barel, A.V., Vandewalle, S.: Robust optimization of PDEs with random coefficients using a multilevel Monte Carlo method. *SIAM/ASA J. Uncertain. Quantif.* **7**(1), 174–202 (2019)
- [20] Borzi, A., von Winckel, G.: Multigrid methods and sparse-grid collocation techniques for parabolic optimal control problems with random coefficients. *SIAM J. Sci. Comput.* **31**(3), 2172–2192 (2009)
- [21] Ge, L., Sun, T.: A sparse grid stochastic collocation discontinuous Galerkin method for constrained optimal control problem governed by random convection dominated diffusion equations. *Numer. Func. Anal. Optim.* **40**, 763–797 (2019)
- [22] Sun, T., Shen, W., Gong, B., Liu, W.: A priori error estimate of stochastic Galerkin method for optimal control problem governed by stochastic elliptic PDE with constrained control. *J. Sci. Comput.* **67**, 405–431 (2016)
- [23] Dürrwächter, J., Kuhn, T., Meyer, F., Schlachter, L., Schneider, F.: A hyperbolicity-preserving discontinuous stochastic Galerkin scheme for uncertain hyperbolic systems of equations. *J. Comput. Appl. Math.* **370**, 112602 (2020)
- [24] Fishman, G.S.: Monte Carlo: Concepts, Algorithms, and Applications. Springer, New York (1996)

- [25] Liu, J.S.: Monte Carlo Strategies in Scientific Computing. Springer Series in Statistics. Springer, New York (2008)
- [26] Xiu, D., Karniadakis, G.E.: The Wiener–Askey polynomial chaos for stochastic differential equations. *SIAM J. Sci. Comput.* **24**(2), 619–644 (2002)
- [27] Poëtte, G., Després, B., Lucor, D.: Uncertainty quantification for systems of conservation laws. *J. Comput. Phys.* **228**(7), 2443–2467 (2009)
- [28] Öffner, P., Glaubitz, J., Ranocha, H.: Stability of correction procedure via reconstruction with summation-by-parts operators for Burgers’ equation using a polynomial chaos approach. *ESAIM: M2AN* **52**(6), 2215–2245 (2018)
- [29] Leykekhman, D., Heinkenschloss, M.: Local error analysis of discontinuous Galerkin methods for advection-dominated elliptic linear-quadratic optimal control problems. *SIAM J. Numer. Anal.* **50**(4), 2012–2038 (2012)
- [30] Yücel, H., Benner, P.: Adaptive discontinuous Galerkin methods for state constrained optimal control problems governed by convection diffusion equations. *Comput. Optim. Appl.* **62**, 291–321 (2015)
- [31] Yücel, H., Heinkenschloss, M., Karasözen, B.: Distributed optimal control of diffusion-convection-reaction equations using discontinuous Galerkin methods. In: *Numer. Math. Adv. Appl.* 2011, pp. 389–397. Springer, Berlin (2013)
- [32] Arnold, D.N., Brezzi, F., Cockburn, B., Marini, L.D.: Unified analysis of discontinuous Galerkin methods for elliptic problems. *SIAM J. Numer. Anal.* **39**(5), 1749–1779 (2002)
- [33] Rivière, B.: *Discontinuous Galerkin Methods for Solving Elliptic and Parabolic Equations. Theory and Implementation.* *Frontiers Appl. Math.* SIAM, Philadelphia (2008)
- [34] Saad, Y., Schultz, M.H.: GMRES a generalized minimal residual algorithm for solving nonsymmetric linear systems. *SIAM J. Sci. Stat. Comp.* **7**, 856–869 (1986)
- [35] Ballani, J., Grasedyck, L.: A projection method to solve linear systems in tensor product. *Numer. Linear Algebra Appl.* **20**, 27–43 (2013)
- [36] Kressner, D., Tobler, C.: Low-rank tensor Krylov subspace methods for parametrized linear systems. *SIAM J. Matrix Anal. Appl.* **32**(4), 1288–1316 (2011)

- [37] Stoll, M., Breiten, T.: A low-rank in time approach to PDE-constrained optimization. *SIAM J. Sci. Comput.* **37**(1), 1–29 (2015)
- [38] Benner, P., Dolgov, S., Onwunta, A., Stoll, M.: Low-rank solvers for unsteady Stokes–Brinkman optimal control problem with random data. *Comput. Methods Appl. Mech. Engrg.* **304**, 26–54 (2016)
- [39] Benner, P., Dolgov, S., Onwunta, A., Stoll, M.: Low-rank solution of an optimal control problem constrained by random Navier–Stokes equations. *SIAM J. Sci. Comput.* **91**(11), 1653–1678 (2020)
- [40] Garreis, S., Ulbrich, M.: Constrained optimization with low-rank tensors and applications to parametric problems with PDEs. *SIAM J. Sci. Comput.* **39**, 25–54 (2017)
- [41] Lions, J.-L.: *Optimal Control of Systems Governed by Partial Differential Equations*. Springer, Berlin (1971)
- [42] Tröltzsch, F.: *Optimal Control of Partial Differential Equations: Theory, Methods and Applications*. Graduate Studies in Mathematics, vol. 112. American Mathematical Society, Providence, RI (2010)
- [43] Babuška, I., Tempone, R., Zouraris, G.E.: Galerkin finite element approximations of stochastic elliptic partial differential equations. *SIAM J. Numer. Anal.* **42**(2), 800–825 (2004)
- [44] Lord, G.J., Powell, C.E., Shardlow, T.: *An Introduction to Computational Stochastic PDEs*. Cambridge University Press, New York (2014)
- [45] Wiener, N.: The homogeneous chaos. *Amer. J. Math.* **60**, 897–938 (1938)
- [46] Karhunen, K.: Über lineare Methoden in der Wahrscheinlichkeitsrechnung. *Ann. Acad. Sci. Fennicae. Ser. A. I. Math.-Phys.* **1947**(37), 79 (1947)
- [47] Loève, M.: Fonctions aléatoires de second ordre. *Revue Sci.* **84**, 195–206 (1946)
- [48] Babuška, I., Chatzipantelidis, P.: On solving elliptic stochastic partial differential equations. *Comput. Methods Appl. Mech. Engrg.* **191**(37–38), 4093–4122 (2002)
- [49] Powell, C.E., Elman, H.C.: Block-diagonal preconditioning for spectral stochastic finite-element systems. *IMA J. Numer. Anal.* **29**(2), 350–375 (2009)
- [50] Øksendal, B.: *Stochastic Differential Equations*. Springer, Berlin (2003)

- [51] Cameron, R.H., Martin, W.T.: The orthogonal development of non-linear functionals in series of Fourier-Hermite functionals. *Ann. of Math. (2)* **48**, 385–392 (1947)
- [52] Ernst, O.G., Ullmann, E.: Stochastic Galerkin matrices. *SIAM J. Matrix Anal. Appl.* **31**, 1848–1872 (2010)
- [53] Barth, A., Stein, A.: Numerical analysis for time-dependent advection diffusion problems with random discontinuous coefficients. *ESAIM: M2AN* **56**(5), 1545–1578 (2022)
- [54] Çiloğlu, P., Yücel, H.: Stochastic discontinuous Galerkin methods with low-rank solvers for convection diffusion equations. *Appl. Numer. Math* **172**, 157–185 (2022)
- [55] Li, R., Liu, W., Ma, H., Tang, T.: Adaptive finite element approximation for distributed elliptic optimal control problems. *SIAM J. Control Optim.* **41**(5), 1321–1349 (2002)
- [56] Akman, T., Yücel, H., Karasözen, B.: A priori error analysis of the upwind symmetric interior penalty Galerkin (SIPG) method for the optimal control problems governed by unsteady convection diffusion equations. *Comput. Optim. Appl.* **57**, 703–729 (2014)
- [57] Meidner, D., Vexler, B.: A priori error estimates for space-time finite element discretization of parabolic optimal control problems. I. Problems without control constraints. *SIAM J. Control Optim.* **47**(3), 1150–1177 (2008)
- [58] Zhou, Z., Yan, N.: The local discontinuous Galerkin method for optimal control problem governed by convection diffusion equations. *Int. J. Numer. Anal. Model.* **7**(4), 681–699 (2010)
- [59] Adams, R.A.: *Sobolev Spaces*. Academic Press, Orlando, San Diego, New-York (1975)
- [60] Bergounioux, M., Ito, K., Kunisch, K.: Primal-dual strategy for constrained optimal control problems. *SIAM J. Control Optim.* **37**(4), 1176–1194 (1999)
- [61] Benner, P., Breiten, T.: Low rank methods for a class of generalized Lyapunov equations and related issues. *Numer. Math.* **124**(3), 441–470 (2013)
- [62] Freitag, M.A., Green, D.L.H.: A low-rank approach to the solution of weak constraint variational data assimilation problems. *J. Comput. Phys.* **357**, 263–281 (2018)

- [63] Lee, K., Elman, H.C.: A preconditioned low-rank projection method with a rank-reduction scheme for stochastic partial differential equations. *SIAM J. Sci. Comput.* **39**(5), 828–850 (2017)
- [64] Benner, P., Onwunta, A., Stoll, M.: Low-rank solution of unsteady diffusion equations with stochastic coefficients. *SIAM/ASA J. Uncertain. Quantif.* **3**, 622–649 (2015)
- [65] Gunzburger, M., Ming, J.: Optimal control of stochastic flow over a backward-facing step using reduced-order modeling. *SIAM J. Sci. Comput.* **33**(5), 2641–2663 (2011)
- [66] Chen, P., Quarteroni, A.: Weighted reduced basis method for stochastic optimal control problems with elliptic PDE constraint. *SIAM/ASA J. Uncertain. Quantif.* **2**, 364–396 (2014)